

# **QUANTITATIVE DYNAMIC RESILIENCE ASSESSMENT OF CHEMICAL PROCESS UNITS USING DYNAMIC BAYESIAN NETWORK**

**Altyngul Zinetullina**

Bachelor of Engineering in Chemical Engineering

**Submitted in fulfillment of the requirements for the degree of Master  
of Science in Chemical and Materials Engineering**



**School of Engineering**

**Department of Chemical and Materials Engineering**

**Nazarbayev University**

53 Kabanbay Batyr Avenue,

Nur-Sultan, Kazakhstan, 010000

**Supervisor:** Dr. Ming Yang

**Co-Supervisor:** Dr. Boris Golman

**April 2020**

# Abstract

Chemical process systems are becoming more and more sophisticated and complex. This makes it more challenging to identify the causes of system failures and perform the process safety analysis. In most cases, accidents happen at the level of socio-technical interactions, and the emerging hazards of these systems cannot be wholly identified and are highly uncertain. Resilient process systems can better handle uncertain hazards and failure scenarios. The dynamic resilience assessment facilitates the identification of the critical factors affecting resilience during the pre- and post-failure phases in a temporal manner. This, in turn, facilitates the identification of the root causes of the accident, timely prevention of it, and employment of useful and specific safety measures.

This study has made a first attempt to use a Bow-Tie (BT) model as a tool to perform accident scenario analysis, and then the BT was converted to DBN for dynamic resilience assessment. This process facilitates the identification of the functionality state of the system and the critical factors affecting the resilience state of the system. Quantitative resilience assessment should be further enhanced for identification of the root causes of the accident on the level of socio-technical interactions and development of the specific resilience attributes to withstand or recover from the highly probable disruption factors. This approach is believed to ensure complex process system safety and functionality. The current study also investigates the opportunity of integrating Functional Resonance Analysis Method (FRAM) and Dynamic Bayesian Network (DBN) for quantitative resilience assessment to identify the highly probable disruption factors and to develop the corresponding resilience attributes.

The proposed method is demonstrated through case studies on a two-phase separator of the acid gas sweetening unit: operating at standard ambient conditions( Case Study 2) and operating at harsh cold conditions (Case Study 1). The analysis of the resilience state of the process system at the worn-out conditions is also done for each case study. The study also integrates Aspen Hysys simulation for the probability of failure (POF) generation. The outcomes of this research provide a rigorous dynamic quantitative resilience analysis approach for complex process systems on the level of socio-technical interactions and a tool for identification of the critical factors or safety measures that enhance the resilience state of the chemical process system.

# Acknowledgements

I would like to express my deepest gratitude to my research supervisor Dr Ming Yang for all the support, knowledge, understanding and opportunities to develop he provided from the first days of our joint work.

I would like to also thank the co-supervisor Dr Boris Golman for his advices, knowledge, and experience that he shared with me throughout the development of this project.

Furthermore, I feel grateful for all the opportunities, courses, faculty, and facilities provided by my Alma-Mater Nazarbayev University throughout the study period. I also want to acknowledge Young Researches Association who funded the conference on Process Safety and Big Data in Frankfurt, Germany, where I presented the part of this research work.

Finally, I am expressing my deepest gratitude to my family who always believed in me and supported me morally whenever I needed it.

# Table of Contents

<b>Abstract</b>	ii
<b>Acknowledgements</b>	iii
<b>Table of contents</b>	iv
<b>List of Abbreviations &amp; Symbols</b>	vi
<b>List of figures</b>	vii
<b>List of tables</b>	viii
 Chapter 1 - Introduction	 1
1.1 Background and problem statement	1
1.2 Motivation of the research	3
1.3 Objective	3
1.4 Thesis Structure	4
 Chapter 2 – Literature Review	 5
2.1 Concept of resilience	5
2.2. Previous work on resilience assessment	6
 Chapter 3 – Dynamic QRA of the separator at the harsh cold conditions: use of BT and DBN approach.	 9
3.1 The proposed methodology for BT to DBN conversion model for resilience assessment of chemical process systems at the harsh environmental conditions	11
3.1.1 Identify the absorption, adaption and restoration parameters	12
3.1.2 Construct the BT diagram	12
3.1.3 Map BT to DBN	13
3.1.4 Estimate the probabilities of reliability states of the system by running the DBN model	13
3.1.5 Develop the Dynamic Resilience Curve	13
3.1.6 Revise the design of the Process System to improve the resilience	14
3.1.7 Reassess the resilience of the system and compare with the previous resilience curve	14
3.2 Case Study 1	18
3.2.1 Development of the DBN model	18
3.2.2 Resilience assessment using the DBN model	25
3.2.3 Design for a more resilient system	27
3.2.4 Posterior Analysis	30
3.2.5 Sensitivity analysis	31

Chapter 4 – Dynamic QRA of separator at standard ambient conditions: integration of FRAM and DBN approach.	33
4.1 The proposed methodology for dynamic resilience assessment with FRAM and DBN integration	33
4.1.1 Development of the FRAM model	35
4.1.2 Development of the FRAM model	37
4.1.3 Preliminary development of the DBN model based on the most critical coupling	40
4.1.4 Application of simulation to the extraction of POFs	40
4.1.5 Reassessment of the Resilience Curve with the inclusion of additional safety measures in the DBN model	41
4.1.6 Sensitivity Analysis for identification of the most influential nodes	41
4.1.7 The assessment of the resilience profile of worn-out equipment	41
4.2 Case Study 2	42
4.2.1 FRAM Analysis	42
4.2.2 DBN Model	44
4.2.3 Application of simulation for extraction of POFs	45
4.2.4 Sensitivity Analysis in Genie Simulation for identification of the most influential nodes	52
4.2.5 The Worn-Out Separator Reliability Assessment	53
Chapter 5 - Conclusion and future work	55
<b>Bibliography</b>	57

# List of Abbreviations & Symbols

BT	Bow- Tie
CO <sub>2</sub>	Carbon dioxide
CPT	Conditional Probability Table
$CV_{ij}$	Cumulative variability
DBN	Dynamic Bayesian Network
DEA	Diethanolamine
E	New observation
FMEA	Failure Mode and Effect Analysis
FRAM	Functional Resonance Analysis Method
FWKO TK	Free Water Knockout Tank
H <sub>2</sub> S	Hydrogen disulfide
MCS	Monte Carlo Simulation
MTBF	Mean time between failure
MTTR	Meantime to repair
OV	Overall variability
$P(X_i^t)$	Parent node
$P(X^t)$	Joint Probability of conditional nodes
$P(X E)$	Posterior probability
PLC	Programmable Logic Computers
POF	Probabilities of failure
QRA	Quantitative Resilience Assessment
$R(t)$	Reliability value after a certain time t
S1	The normal state at time $t_1$ when the disruption occurs
S2	The state with the lowest functionality due to disruption occurrence at time $t_2$
S3	The state of the system after the adaptation stage at time $t_3$
S4	The recovered state of the system after restoration is finished at time $t_4$
SADT	Structured Analysis and Design Technique
SIS	Safety Instrumented Systems
SME	Subject Matter Expert
t	time
TK	Tank
$V_j^T$	Variabilities of upstream functions based on timing
$V_j^P$	Variabilities of upstream functions based on precision
VLV	Valve
$\alpha_{ij}^T$ and $\alpha_{ij}^P$	Amplification factors based on the timing and precision
$\beta$	Shape parameter
$\lambda$	Constant failure rate, the inverse of the mean time between failure
$\mu$	Repair rate, the inverse of the meantime to repair
$\eta$	Scale parameter

# List of figures

Figure 3.1. Acid gas sweetening unit modelled in Aspen Hysys	10
Figure 3.2. The proposed method for dynamic resilience assessment	11
Figure 3.3. The state change of system functionality	15
Figure 3.4. A transformation from the Markov chain model to DBN for illustration of change of the functionality of a system	16
Figure 3.5. Simplified DBN model in GeNIe	16
Figure 3.6. The fault tree constituent of the BT diagram	20
Figure 3.7. The event tree constituent of the BT diagram	21
Figure 3.8. The DBN model for resilience assessment	22
Figure 3.9. The dynamic probability profile of four functionality states	26
Figure 3.10. The dynamic change of the separator's resilience	26
Figure 3.11. The new DBN model (with additional nodes) for resilience assessment of a separator	28
Figure 3.12. The resilience of the separator with new design	28
Figure 3.13. The resilience profile obtained as a result of the posterior analysis	30
Figure 4.1. The proposed methodology for dynamic resilience assessment	34
Figure 4.2. Acid gas sweetening unit modelled in Aspen Hysys	42
Figure 4.3. FRAM Model for the activities related to the 2-phase separator	43
Figure 4.4. Developed DBN model for the identified critical path	45
Figure 4.5. Process control of the 2-phase separator	46
Figure 4.6. Valve VLV- 102 actuators have failed open strip chart	46
Figure 4.7. Level controller incorrectly set-up due to wrong switch selection	47
Figure 4.8. Simulation of fire in the 2-phase separator	48
Figure 4.9. The Resilience curve	49
Figure 4.10. Updated DBN model with the additional parameters	50
Figure 4.11. The resilience model of the system with additional resilience parameters	50
Figure 4.12. The resilience profile of the worn-out separator	54

# List of tables

Table 3.1 Transition rates of the Markov chain	16
Table 3.2. Basic Events of the Fault Tree and respective Probabilities	19
Table 3.3. External and Internal Disruptions	22
Table 3.4. The parent and child nodes used for resilience modelling	23
Table 3.5. The classification of consequences in the BT and their association with functionality state	24
Table 3.6. Transition rates for assigning the conditional probabilities of resilience states	25
Table 3.7. Additional parameters	27
Table 3.8. Comparison of resilience metrics	29
Table 3.9. Pieces of evidence for selected nodes	30
Table 3.10. Comparison of prior and posterior Resilience parameters	31
Table 3.11. The scenarios used for sensitivity analysis	32
Table 3.12. The results of the Sensitivity Analysis	32
Table 4.1. Variability scoring based on Timing and Precision	38
Table 4.2. Discrete Probabilities Distributions for Timing variabilities	38
Table 4.3. Discrete Probabilities Distributions for Precision variabilities	38
Table 4.4. The ranges for amplification factors	39
Table 4.5. The FRAM couplings with indicated amplification factors	44
Table 4.6. Additional safety measures for the DBN model	50
Table 4.7. Comparison of resilience metrics	51
Table 4.8. Scenarios for sensitivity analysis	52
Table 4.9. The results of sensitivity analysis	53



# Chapter 1 - Introduction

## 1.1 Background and problem statement

The technology is moving forward and the process safety measures are increasingly becoming automated to facilitate the safe environment in the chemical process plants. However, the automation has also led to complexities and accident occurrence on the level of the socio-technical interactions. The goal of the industrial plants nowadays is not only preventing the accidents but also dealing with the daily disturbances and variabilities even after their occurrence to sustain the system in the normal operational state. Hence, the goal of the industrial system management is to have not rigid but more flexible and resilient systems (Hollnagel et al., 2006; Steen and Aven, 2011).

The research study addresses the solutions for two main problems faced in the industrial safety engineering.

- 1) The traditional risk assessment methods employed in the industry focus on the measures to prevent accidents only (Park et al, 2013).

Although it is important to accommodate the measures to avoid the accidents, it is also crucial to examine and supplement the equipment with the measures for the recovery of the equipment from failure. Therefore this study will develop the dynamic quantitative resilience assessment method. The resilience assessment allows us to monitor the ability of the system to avoid the accident occurrence, and in the case when an accident happened to recover from it. Thus, the current ability and amount of time for the system recovery could be analyzed. Taking into account the effectiveness of the post-accident scenarios can result in the safe and fast recovery of the operating system with minimal or no losses. Therefore this study will develop the dynamic quantitative resilience assessment method. The resilience assessment allows us to monitor the ability of the system to avoid the accident occurrence, and in the case when an accident happened to recover from it. Thus, the current ability and amount of time for the system recovery would be analyzed. Taking into account the effectiveness of the post-accident scenarios can result in the safe and fast recovery of the operating system with minimal or no losses.

- 2) The industry employs various safety measures and automated complex equipment to reach zero accidents. However, this goal is still unattainable. The complexity of

equipment and the indirect causes of the accident as the human factors or organizational factors may result in unpredictable equipment failures, that may escalate into the major accidents under the impact of domino effect (Patriarca et. al, 2017). Therefore this study will present the method to identify the most vulnerable socio-technical interactions of the system beforehand to either avoid the accident from happening or to enhance its recovery properties. Therefore this study will present the method to identify the most vulnerable socio-technical interactions of the system beforehand to either avoid the accident from happening or to enhance its recovery properties.

In this study, the four attributes of the resilience will be used to build a model to quantify resilience based on the definition - “the probability of a system’s functionality state sustaining a “high functionality” state or restoring to a “high functionality” state from a “low functionality” state during and after the occurrence of disruptions in the operation of a system within a specific time.” (Tong and Yang, 2020). Functionality represents the capability of the system to perform its prescribed functions. The state of functionality of the system could be classified as “high” or “low”, where high functionality state refers to the capability of the system to perform all its functions. In contrast, a low functionality state refers to the inability to perform the majority of all the required functions or perform but at a reduced level (Birolini, 2013).

In this study, the two approaches for the resilience assessment will be analyzed. The first approach will assess the resilience of the system for the specific threat, set by the user. In this case, the resilience of the winterization measure (i.e., electrical heat tracing) on the installations of the acid gas sweetening unit (i.e., separator) will be assessed using the generic resilience assessment method proposed in (Tong and Yang, 2020) with the integration of BT and DBN. The method was universalized to the power loss or overcurrent issues that could happen to any heat-traced process units operating in harsh cold environments. The second approach will be based on finding the root cause of the possible accident and further assessment of the resilience of the system for these causes using the FRAM and DBN models. The dynamic quantitative resilience assessment of the installations will be accomplished via the integration of the qualitative (BT) model and quantitative DBN.

The study will also analyze the system performance under harsh cold conditions. For the same system operating in a temperate region, the effects of hazards are amplified by the harsh environmental conditions, such as icing, snowstorms, strong winds, darkness, and remoteness to emergency support bases (Naseri, 2017). The resilience assessment is essential

for process systems operating in harsh environments due to their impacts on systems' performance, lack of knowledge and operational experience, limited resources available for emergency responses due to remoteness. Under the harsh cold conditions, the system will operate at or close to its design limits. This significantly reduces the lifetime of the equipment and increases the probability of system failure (Naseri, 2017). Winterization could be the most prominent measure to increase the reliability of the system and minimize the disruption possibility and effects in a harsh cold environment. Standard winterization measures include but not limited to insulation, heat tracing, de-icing equipment, chemical seals, antifreeze additives, and ice-repellent coatings (Yang et al., 2013). Malfunction of one of the winterization methods applied to the system may lead to the operational instability, consequent system outage, the occurrence of cascading abnormal events, finally, may result in a severe accident. Thus, minimization of human factors and enhancing the functionality of winterization measures would help to build more resilient systems in harsh cold environments.

## **1.2 Motivation of the research**

Previous works considered resilience as a static property of the system, which seems an oversimplified assumption for complex process systems experiencing disturbances continuously throughout their daily operation. Furthermore, conventional risk assessment methods that are used for the safety assessment of systems are not enough because their application is restricted mainly to the accident prevention phase, not to the response of the system after the accident occurrence (Tong and Yang, 2020). Resilience assessment is focused on the both accident prevention and the recovery from the accident in the dynamic manner. Therefore, the motivation of this work is in developing the tool for the dynamic resilience assessment of the chemical process system under standard and extreme ambient environment. The tool will be helpful to identify the most vulnerable components of the system including the socio-technical constituents of it and will be able to assess the resilience of the system for both specified and unspecified threats. Furthermore, the tool will facilitate the identification of the critical safety measures enhancing the resilience of the system.

Overall, the output of this work will be helpful to reduce the risk of accident occurrence, or in case if it is occurred to enhance and expedite the recovery of the process system.

### 1.3 Objectives

Risk assessment methods do not consider the post-disruption scenarios and surprises, focusing only on the failure prevention and mitigation measures. To thoroughly study the level of performance of the system and its health condition, it is better to use the dynamic resilience assessment, which considers the state of functionality of the system before and after the disruption effect. This study aims to investigate quantitative dynamic resilience assessment of process facilities, with a focus on the assessment of the system's ability of responding to the disturbance as well as to recover and learn from it using the approaches such as FRAM, BT and DBN for rigorous analysis. The main objectives of this manuscript are:

- To develop a quantitative approach for resilience assessment using dynamic Bayesian network
- To develop an FRAM-based approach to identify the critical factors that affect the system resilience and design for improved resilience
- To test the developed approach for resilience assessment of process systems operating in low temperature environment

### 1.4. Thesis Structure

The remaining part of this manuscript is organized as follows. Chapter 2 presents the Literature Review. Chapter 3 presents the proposed dynamic QRA and its application to the separator at the harsh cold conditions, where for QRA BT and DBN approach is employed. Then, Chapter 4 presents the case study on two-phase separator of the acid gas sweetening unit where FRAM to DBN conversion approach for resilience assessment is implemented. Furthermore, in Chapter 4 the resilience assessment of the separator at worn-out conditions is done.

# Chapter 2- Literature review

## 2.1 Concept of Resilience

In scientific literature, the term resilience first appeared in the materials engineering field to describe the ability of the material to return to the initial shape after deformation (Trautwine, 1919). Then this term was used in the ecological domain as the ability of the ecosystem to sustain the original species by absorption of the changes and disturbances (Holling, 1973). Later, this term started to be used in organizational (Kendra and Wachtendorf, 2003; Burnard and Bhamra, 2011), psychological (Luthar, 2000; Bananno, 2004), economical (Perrings, 2006; Fiksel, 2006; Rose and Liao, 2005), social (Adger, 2000), social-ecological (Gumming et al., 2005; Kinzig et al., 2006) and engineering domains.

In the past decade, resilience has been used in various engineering fields such as water management (Li and Lence, 2007; Vogel and Bolognese, 1995), transportation management (Baroud et al., 2014a, 2014b; Hosseini and Barker, 2016; Faturechi and Hooks, 2014), infrastructure (Berkeley et al., 2010; McCarthy, 2007; Vugrin et al., 2010) and process industries (Azadeh et al., 2014; Dinh et al., 2012; Jain et al., 2018; Shirali et al., 2013). In all of those studies, resilience was defined as the intrinsic property of the system to respond and adjust the functioning before or after a mishap or continuous disturbance to sustain the normal operational performance of the system (Steen and Aven, 2011). According to Hollangel et al. (2007), there are four characteristics that a resilient system should have:

- (1) To provide a strong or flexible response to instant or continuous disturbances;
- (2) To conduct self-monitoring of the system's performance;
- (3) To predict risks and risk development opportunities; and
- (4) To learn from past events.

The more sophisticated definition of the resilience was proposed by Tong et al. (2020), where the resilience was defined as the intrinsic ability of the system to absorb the disruption, or in case if the mishap occurred to adapt to it, restore from it and learn from the experience in a dynamic manner. The authors claimed that resilience was constituted of four attributes, namely absorption, adaptation, restoration, and learning. Furthermore, they discussed the opportunity of dynamic quantification of the resilience with the employment of the Markov Chain and Dynamic Bayesian Network Model. The work of Zinetullina et al. (2019) was a further extension of that work, where the resilience of a process system was identified as a

dynamic state of its functionality. According to Tong et al. (2020) and Zinetullina et al. (2019), resilience is also defined as the ability of the system to sustain high functional state under the effect of disruption or to restore after the disruption from the low functional state to a highly functional state.

Furthermore, the disruption effect at the current time step and the impact of the resilience attributes at the current time step and the previous time steps affect the current state of functionality of the system. The change in the state of functionality induces the change in the resilience of the system. This is because the resilience is the intrinsic ability of the system to perform its functions at the high functionality state

## **2.2 Previous work on resilience assessment**

Resilience engineering application in the process plants is particularly important because of the level of complexity of the equipment, non-linear interconnections and high level of variability and uncertainty arising from this complexity(Costella et al., 2009).

Cai et. al. (2018) considered the performance and time-related properties as the constituents of the resilience. Performance-related properties were robustness, adaptability, and time-related were recoverability, maintainability, etc. The study of Cai et. al (2018) assessed the resilience in terms of availability where high availability and low time to recovery characterizes the high resilience of the system. The availability is considered as the time-dependent term that varies under the impact of disruption failure rate and the effect of the recovery repair rate. The work also employed DBN for the prediction of the future values of availability and their variation with time by employing the data available at the current state. It also conducted a sensitivity analysis to identify the impact on the resilience of disruptive and restorative factors. The conditional probabilities were estimated using the values of repair rate and failure rates. The resilience metric was evaluated based on the availability of components that are connected in series, parallel, and voting systems.

However, the work of Cai et. al. (2018) evaluated the resilience only as a parameter dependent on the failure and repair rates of the consisting components. It considered the occurrence of disruption as the result of the malfunction of some of its technical constituents. However, the failure of the system may occur not only due to technical aspects but also because of the socio-technical aspects of interaction. The assessment includes only the assessment of the resilience based on the availability of its components. The study does not consider the resilience assessment of the system to withstand hazard and when the accident happens to recover from it. Comparatively, in the current study, resilience is considered based on the state

of functionality of the system considering all the technical, social constituents of it as well as the organizational measures involved. In two parts of this study, the resilience of the system to the particular failure is addressed and in the other part the vulnerable point on the level of socio-technical interactions are identified and the resilience of the system is addressed by taking into account probability of failures of its technical constituents and the organization as well as safety measures involved.

The other work of Cai et. al. (2019) conducted remaining useful life (RUL) estimation using DBN. They interpreted the dynamic degradation of the structure by one cause and by multiple causes.

The DBN consisted of the material parameters, crack propagation depth, then the CPTs were filled and RUL was estimated using the time point where the availability of pipeline or reliability decreases to the critical value. Multiple causes were considered there such as fatigue, erosion, internal waves, corrosion. The crack depth of the subsea pipeline was set as a characteristic of the physical performance for the subsea pipeline to calculate the RUL value. First, four DBNs were constructed each representing the DBN models with its characteristic parameters involved for sand erosion, internal waves, fatigue, and corrosion. Then, these four DBNs were joint together at the performance node which was further connected to the evidence node.

In the work of Cai et.al. (2019) DBN model was used for estimation of the RUL and the assessment of the various threats affecting the crack propagation. However, the DBN was used here in terms of the “absorption” or availability properties, but no aspects of the adaptation or recovery from the crack propagation were discussed, as in the present research work.

In the work of Kammouh et.al. (2020) DBN was also used for resilience assessment, where the resilience was described as consisting of three pillars mainly fast recoverability, reduced vulnerability or reduced likelihood of failure and robustness or “reduced consequences of failure” (Bruneau et al, 2003). The resilient system had to have reduced vulnerability, high robustness, and high recoverability. Thus, the paper discussed the resilience as consisting of the stages of pre-disruption, at disruption and post-disruption, where the likelihood of failure referred to the stage of pre-disruption, robustness- to the time of disruption occurrence and the recoverability to the post-disruption stage.

The structuring of the DBN for resilience assessment resembled the structure employed in this paper where the indicator nodes were connected to the resilience attributes and those, in turn, served as the parent nodes for the child node of the resilience index or state of functionality. However, the work failed to provide the detailed network for the damage,

recovery attributes and did not add the learning as the attribute of the resilience. In comparison with this work, the present work allows identifying the root basic causes of the failure occurrence by the integration of the BT and DBN in resilience assessment. Furthermore, the work allows us to identify the most vulnerable socio-technical interconnections of the system in advance and assess the resilience of the system for certain hazards. Additionally, the present work allows adding the supplementary safety measures to the resilience attributes such as adaptation and restoration to assess how this will impact the functionality state of the system with time. Also, the current study includes the opportunity of the system to learn with time and to observe how the learning of the complex system may impact on the resilience of it.

Failure Mode and Effect Analysis (FMEA) methods are not capable of identifying the root causes of the accidents caused by socio-technological interactions; therefore, to deal with the current accidents still occurring in the industry, new safety approaches must be developed. Functional Resonance Analysis Method (FRAM), in comparison with linear FMEA methods, is more capable of predicting the hazards in dynamic and complex systems considering socio-technological interactions of the system components (Patriarca et al., 2017). Resilience is the dynamically changing characteristic of the system. The changes occur with the daily disturbances and variabilities the system undergoes. The current issue with resilience engineering is its incapability of predicting emergent accidents accurately. This happens due to the lack of considering the non-linear interconnections among the system components and their interdependencies with the change of variability (Andersson et al., 2002; Levenson, 2004; Steen and Aven, 2011). Therefore, conducting FRAM analysis at the initial stage of the quantitative resilience assessment of the complex system could facilitate a more rigorous analysis of the operational state of the system and concrete solutions( Rosa et al., 2015). According to Patriarca et al. (2017) and Rosa et al. (2015), FRAM could be considered a viable method for resilience assessment due to two main reasons:

- (1) FRAM identifies the root causes of the level of non-linear socio-technical interactions, which is not possible with any of the current FMEA methods. This approaches the model to the real-life case scenario (Steen and Aven, 2011).
- (2) FRAM model structure consists of activities performed both on and by the system. The resilience parameters can better be characterized by actions of the objects rather than by their presence(Patriarca, Di Gravio, & Costantino, 2017b).

Zinetullina et al. (2019) developed a methodology based on Bow-Tie(BT) and Dynamic Bayesian network (DBN) to quantify the dynamic resilience of process systems. The part of



this work is described in the manuscript for the case of the prescribed accident occurrence. This part will be complemented with the application of FRAM instead of BT for more rigorous analysis of the dynamic resilience of the two-phase separator, where the resilience parameters will be developed for the most vulnerable components of the chemical process system.

DBN is a probabilistic graphical model. It has the same structure and principles as the Bayesian network, with an exception that it allows estimating the joint probabilities of the variables with time. Thus, using DBN allows estimating the joint probabilities at time  $t$ ,  $t+1$ ,  $t+2$  and so on (Jensen & Nielsen, 2007; Neapolitan, 2004).

It consists of the nodes(variables) and arcs, that link the nodes and allow deriving the interdependencies of the nodes based on the conditional probabilities. The nodes are classified as the parent nodes, child nodes and the root nodes. The root nodes are assigned for marginal probabilities the rest are assigned for the conditional probabilities. The joint probability of conditional nodes is calculated at the child node dynamically (2.1) (Jensen & Nielsen, 2007).

$$P(X^t) = P(X_1^t, X_2^t, X_3^t, \dots, X_n^t) = \prod_{i=1}^n P(X_i^t | X_i^{t-1}, pa(X_i^t), pa(X_i^{t-1}), pa(X_i^{t-2}), \dots, pa(X_i^0)) \quad (2.1)$$

In DBN and BN, the joint probability could be updated with the addition of new nodes.

$$P(X|E) = \frac{P(X, E)}{P(E)} = \frac{P(X, E)}{\sum_x P(X, E)} \quad (2.2)$$

Having these characteristics DBN enables predicting the spatial and temporal evolutions of systems probabilistically (Khakzad, 2015). In resilience engineering, it was first applied by Yodo et al (2016) for the assessment of the reliability and restorative properties of the system. However, the limitation of that study was an estimation of restoration only, however, resilience consists of four parameters which are absorption, adaptation, restoration and learning. Furthermore, in his research, the resilience was considered as a constant term, whereas the resilience is a characteristic that changes following the changes of variabilities of components and either internal or external disturbances (Tong et al., 2020).

Furthermore, DBN can be used for both prognostic and diagnostic analyses. Prognostic analysis aims to predict the system performance with time; while the diagnostic analysis is used to identify the most and least effective variables (measures) with regards to the safety, performance, or resilience of the system via sensitivity analysis (Khakzad, 2015).

In the present work, the DBN will be used for the quantification of the dynamic resilience of process systems. The DBN will include nodes to represent the absorption, restoration, adaptation, and learning parameters. Nodes will be structured according to the outcomes of the BT and FRAM analysis. As a result of FRAM the components of the process system having the highest tendency to cause an accident are identified.

Additionally, the study considers the resilience change with time for the worn-out equipment under the effect of gradual corrosion development and, consequently, the equipment walls thinning. The study will use the outcomes of the relevant research works for equipment degradation with time and the developed FRAM to the DBN model for resilience assessment (Liao et al., 2011; Ossai et al., 2015). The Weibull Distribution will be used for the analysis of the equipment degradation.

# **Chapter 3- Dynamic QRA of the separator at the harsh cold conditions: use of BT and DBN approaches**

The following case studies(Chapters 3 and 4) aim to demonstrate the application of the quantitative resilience assessment of a two-phase vertical separator of the acid gas sweetening unit, as shown in Figure 3.1 at winterized (Chapter 3. Case Study 1) and standard conditions (Chapter 4. Case Study 2).

Sour gas treating unit is the part of the oil and gas preliminary treating plant. It accomplishes the absorption of the sour gases (mainly carbon dioxide ( $\text{CO}_2$ ) and hydrogen disulfide ( $\text{H}_2\text{S}$ )) with diethanolamine (DEA) from the gas coming after the crude oil stabilization. Crude oil stabilization is the process during which oil coming from the well is separated into three phases (mainly gas, oil, and water) and the pressure is reduced in stabilizer from high upstream pressure to the normal operating pressures to not harm gas, oil, and water treating process units.

In Figure 3.1, the process flow diagram of the acid gas sweetening is presented. First, sour gas is depleted from process hydrocarbons in two-phase separator FWKO TK. Then, dehydrated sour gas goes to the absorption column wherewith the DEA it depletes from  $\text{CO}_2$  and  $\text{H}_2\text{S}$  and leaves the column as a sweet gas for further production of the sales gas. The “Rich DEA” stream, with  $\text{CO}_2$  and  $\text{H}_2\text{S}$ , then is separated from the hydrocarbons in the separator Flash TK and passes to the Regenerator column, where the products, lean amine, and acid gas are produced. Lean amine stream is refluxed to the absorption column "DEA Contactor" and "Acid Gas" serves as the feed for the Sulfur Recovery Unit (Hysys, 2004).

Developing the way to increase the assurance level of the operations and decrease the number of accidents, near misses and mishaps will secure many lives of the people working in the industry. It will decrease the operational and facility losses. The outcome of this study is the tool for the identification of the root causes of the accident (on the level of socio-technical interactions) and the critical factors improving the resilience of the system as well as the assessment of the resilience state of the system with the safety measures applied dynamically.

Figure 3.1. Acid gas sweetening unit modelled in Aspen Hysys (Hysys,2004)

### 3.1 The proposed methodology for BT to DBN conversion model for resilience assessment of chemical process systems at the harsh environmental conditions

*A version of this chapter has been published in the **Journal of Safety in Extreme Environments** 2019; 1-13. I am the primary author. Co-author Ming Yang provided much needed support in implementing the concept and testing the model. I have carried out most of the data collection and analysis. I have prepared the first draft of the manuscript and subsequently revised the manuscript, based on the feedback from Co-authors and peer review process. The three Co-authors assisted in developing the concept and testing the model, reviewed and corrected the model and results. They also contributed in reviewing and revising the manuscript.*

Figure 3.2 presents the procedure for dynamic resilience assessment while Figure 3.3 schematizes the outcome of the procedure (Tong et al., 2020). In this work, resilience is defined as:

- The probability that the system maintains a “high functionality” state after or during the occurrence of a disruption.
- The probability that the system restores from a “low functionality” state back to a “high functionality” state given a disruption (Tong et al., 2020).

In the following sections, each step of the proposed method will be discussed.

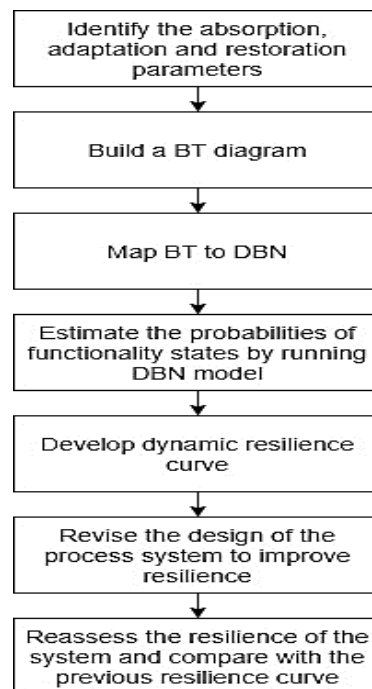


Figure 3.2. The proposed method for dynamic resilience assessment

### ***3.1.1 Identify the absorption, adaption and restoration parameters***

As it was previously stated, the absorption characterizes the ability of the system to sustain the normal operational state or high functionality state after or during the occurrence of disruption by absorbing the destructive impacts on the system. The absorption parameters are characterized by the inherent safety design parameters, such as heat tracing in the present analysis.

Adaptation parameters are auxiliary parts of the system that return the system to the normal operational state automatically. This could be the process safety equipment such as the safety relief valves, temperature controllers, and flow controllers.

Restoration parameters are characterized by the external forces that return the system to the normal operational state. This could be maintenance works, an update of the safety procedure, and organizational management rules. The identified parameters are then used to construct a bow-tie diagram.

### ***3.1.2 Construct the BT diagram***

Bow-Tie analysis is a graphical approach that enables observing the development of a system's malfunction scenarios (i.e., Top Event) starting from the root causes and finishing with the consequences (Zhang et al., 2018). It consists of a fault tree and an event tree. In the fault tree, the root and intermediate causes of the malfunction are disclosed, whereas in the event tree, the consequences are identified based on the combination of success and failure of the safety barriers. The disadvantage of the BT approach is its inability to present the dynamic representation of the probabilities and incapability to update the probabilities with new information entered (Zhang et al., 2018). Therefore, in this study, BT will be mapped into DBN to quantify the resilience.

The BT diagram was constructed by simulating the failure of the absorption parameters in the fault tree part. The adaptation and restoration parameters were inserted into the event tree part as the safety barriers.

### 3.1.3 Map BT to DBN

For mapping BT to DBN, the absorption, adaptation, and restoration parameters were extracted and presented as the “Absorption”, “Adaptation” and “Restoration” nodes accordingly. The three abovementioned nodes with the “Learning” node were connected to the “State of Functionality” node. The Conditional Probability Tables (CPTs) of the nodes are then filled with the probabilities of failure and success based on the estimations done with the Markov Model, literature data, and expert judgment.

For the nodes in DBN two states were assigned in CPTs, which are “High Functionality” and “Low Functionality”. As the CPTs of nodes “Absorption”, “Adaptation” and “Restoration” consist of the different combinations of the state of functionalities of the corresponding nodes, the conditional probabilities were assigned based on the expert judgement for each separate scenario. Starting from the highest conditional probability where all constituting nodes have the high functionality and finishing with the lowest conditional probability for the case when each constituting node has low functionality state.

For CPT of node “State of Functionality” the CPT from the work of Tong et. Al. (2020) was used. For the time at disruption  $t=0$ , S1- state of functionality at the disruption, was assigned the value of 1, and the states S2, S3, S4 were equated to zero. For time  $t=t+1$ , the Fuzzy Analytical Hierarchy Process (FAHP) was used to fill the conditional probabilities table. Then, the weights were assigned based on the 30 expert’s judgement after comparison of the pairwise parameters based on the triangular fuzzy conversion scale. Then the assigned scores were converted into the probabilities with the employment of the Chang’s extent analysis method. For more details please refer to the work of Tong et. al. (2020).

The other nodes except node “State of functionality” were not represented as the dynamic ones because the information for those was specified for the current state. Further, the Genie estimated the variation of the “State of functionality” node with time by employing DBN. The estimations of the future functionality of the data was done by employing the current present data. The simulation tried to replicate the real case scenarios when you have your current data and make predictions for the future estimations.

### ***3.1.4 Estimate the probabilities of reliability states of the system by running the DBN model***

The GeNIe Simulation estimates the joint probability of the functionality state based on eqn 1 for the time steps in the specified time interval (Genie, n.d.). The resultant probability versus time steps curve is presented in Figure 3.3. S1, S2 S3, and S4 represent the states of the system functionality. S1 represents the initial state of the system at the time( $t_1$ ) when the disruption occurred. After the disruption occurrence, the state of the system functionality drops, resulting in the state of the low functionality at the state S2 and S3. Adaptation and restoration stages of the system occur at the S2 and S3 stages of the system. The impact of the adaptation and restoration parameters on the system performance finally results in the recovery of the system to the normal operational state or the high functionality of the system state, i.e., S4.

### ***3.1.5 Develop the Dynamic Resilience Curve***

The dynamic resilience curve, as presented in Figures 3.3, is derived based on the addition of the initial state (S1) of the system's functionality and the final recovered functionality state of the system (S4). This idea was previously proposed by Yodo et al. (2017), however, without considering the transient variation of the probability. The dynamic variation of the probability changes for the sum of states S1+S4 was developed by Tong et al. (2020) and is implemented in the present study.

According to Holling (1973), the initial state of the system, before the occurrence of disruption was denominated by S1 in Figure 3.3. In this figure, the decline of the functionality state is represented by the graph between states S1 and S2; adaptation is represented by the change from S2 to S3; and restoration is shown by the change from S3 to S4; and the learning can contribute to both state change from S2 to S3 and S3 to S4. S4 represents the new normal operational state of the system. The high learning capability of the system designates that the absorption, adaptation, and restoration will have high capacity or, consequently, higher resilience if the disruption occurs. Thus, S1 state of functionality could be less than S4, because S1 characterizes the state the system had at the time of disruption, and S4 characterizes the state of functionality the system has after the adaptation and restoration stages. Thus, if the disruption occurred, then the system did not have strong resilience properties and high functionality, S4 characterizes the state after the works were completed to enhance the resilience of the given system.



At this step of the analysis, time for 90% recovery is also identified. 90% recovery time refers to the time for 90 % recovery of the lost resilience or the lost functionality after the destruction. 90% was assumed as acceptable resilience level in this study.

### ***3.1.6 Revise the design of the Process System to improve the resilience***

At this stage, the resilience of the system is observed after the addition of the resilience parameters for each node "Absorption", "Adaptation", "Restoration" correspondingly. The increase of the resilience of the system with the addition of the safety measures partially validates the usefulness of the built model. The increase of the system resilience is characterized by the longer time to reach the lowest probability of the state of the system's functionality, a higher value of the lowest probability, increased or the same probability of having the high functionality state after the adaptation and restoration stages.

The longer time to reach the lowest probability and a higher value of the lowest probability characterizes the strong absorption characteristics of the designed system. At the same time, having the system returned to the normal operational state designates both the ability of the system to restore and the effectiveness of the adaptation and restoration parameters.

### ***3.1.7 Reassess the resilience of the system and compare with the previous resilience curve***

The resilience of the system is reassessed by conducting sensitivity analysis on the nodes that exert the highest impact on the state of reliability of the system, or critical nodes. After the critical nodes are identified, the pieces of evidence at time slots are implemented in the DBN. The resilience change due to these implementations is also checked. It is necessary to understand which parameters contribute to the highest drop of the functionality due to disruption or which parameters result in a faster recovery to the normal operational state. This helps with the enhancement of inherently safe design. The limited resources can be appropriately allocated to the improvement of the critical factors for system resilience. It can also help to identify and implement the most impactful adaptation and restoration parameters to improve system resilience.

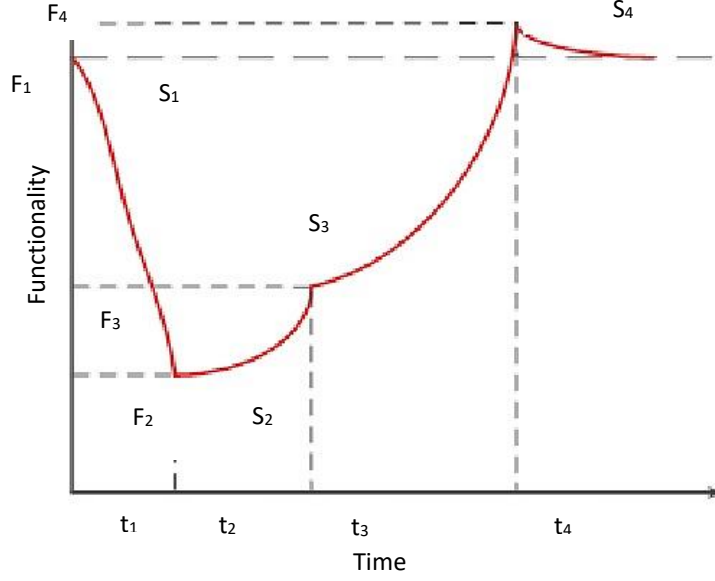


Figure 3.3. The state change of system functionality (Tong et al., 2020).

In the work of Tong et al. (2020), the four states are quantified by application of the Markov Chain Model using parameters presented in Table 3.1. The  $\lambda_1, \mu_1, \mu_2, \lambda_2$  are the transition probabilities referring to absorption, adaptation, restoration, and learning correspondingly (Figure 3.4) (Tong et al., 2020).

The states in the Markov Model are defined in the following way:

- S1: The normal state at time  $t_1$  when the disruption occurs
- S2: The state with the lowest functionality due to disruption occurrence at time  $t_2$
- S3: The state of the system after the adaptation stage at time  $t_3$
- S4: The recovered state of the system after restoration is finished at time  $t_4$ .

As presented in Figure 2.3 the transitions from states S1 to S2, S2 to S3, S3 to S4 and S4 to S1 are characterized with the transitional probabilities  $\lambda_1, \mu_1, \mu_2, \lambda_2$  correspondingly.

There  $\lambda$  – constant failure rate, the inverse of the mean time between failure(MTBF),  $\lambda = \frac{1}{MTBF}$ , and  $\mu$ - repair rate, the inverse of the meantime to repair,  $\mu = \frac{1}{MTTR}$  (Tong et al., 2020).

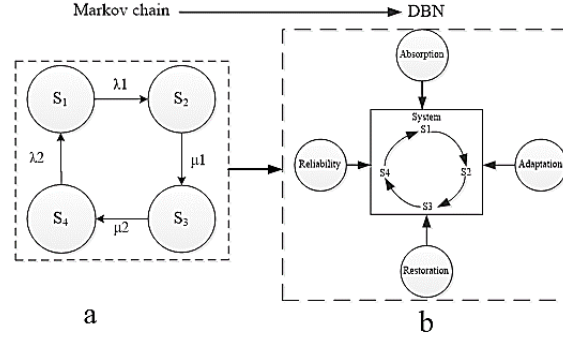


Figure 3.4. A transformation from the Markov chain model to DBN for illustration of change of the functionality of a system: (a) Markov chain model; (b) DBN.

Table 3.1. Transition rates of the Markov chain (Tong and Yang, 2019)

Transition probability	$S_1$	$S_2$	$S_3$	$S_4$
$S_1$	$1 - \lambda_1$	$\lambda_1$	0	0
$S_2$	0	$1 - \mu_1$	$\mu_1$	0
$S_3$	0	0	$1 - \mu_2$	$\mu_2$
$S_4$	$\lambda_2$	0	0	$1 - \lambda_2$

The obtained values for  $S_1$ ,  $S_2$ ,  $S_3$ , and  $S_4$  are then used in the Conditional Probability Table (CPT) of node “State of Functionality” in the DBN model (Figure 3.5).

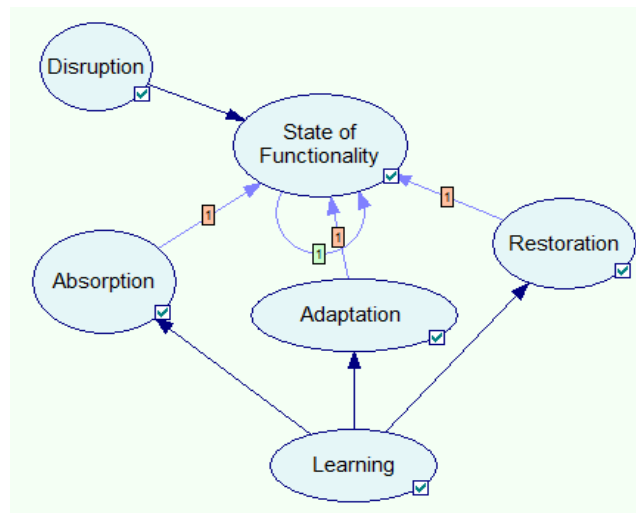


Figure 3.5. Simplified DBN model in GeNIe (Tong et al., 2020)

In Figure 3.5, the generic DBN model for quantifying resilience is displayed. It consists of six nodes: child node (leaf node) - "State of Functionality" and five parent nodes: "Disruption", "Absorption", "Adaptation", "Restoration" and "Learning". "Learning" is a parent node for nodes "Absorption", "Adaptation", "Restoration". This designates that the Learning ability of the system affects the ability of the system to absorb failure, adapt to disruption, and restore from it after the subsequent mishap (Tong et al., 2020). "Disruption" node characterizes external and internal factors that may facilitate the malfunction and the decrease of the functional reliability of the system if the absorption was not high enough to confront the disruption effects.

The joint probability of the "State of the Functionality" node is calculated based on eqn. 3.2, and it assumes that the probabilities of the system and contributing factors at the time (t-1) influence the resilience of the system at time t. The Transient resilience model (Figure 3.3) is obtained by adding the probabilities of S1 and S4 calculated using DBN (Tong and Yang, 2019).

### 3.2 Case Study 1

#### 3.2.1 Development of the DBN model

The proposed method was applied to the resilience assessment of a separator system with electric heat tracing operating in the harsh cold conditions. According to an experienced operator, the main disruption to this system is the failure of the self-regulating electric heat tracing. The failure may lead to a rapid decrease in the operating temperature of the separator, causing wax and hydrate formation on the separator, which could impair its operation and create blockages of process piping. In such cases, the adaptation and restoration components of the system will be activated that can be modelled as safety barriers in the Bow-Tie analysis. The Bow Tie was developed for this case as in Figures 3.6 and 3.7.

The leading causes of the failure of the electrical heat tracing were identified through literature review and an interview with an operator who has vast experience of operations in harsh cold environments. These causes are the power loss (particularly the outage of the main power generator and the standby generator), overcurrent protection and residual current device tripping. These causes were further reasoned by other intermediate causes ending up with the root (basic) causes (Table 3.2).

Table 3.2. Basic Events of the Fault Tree and respective Probabilities

Acronyms	Basic Events	Probabilities
A	Anxiety	0.091
CWC	Cold Weather Conditions	0.091
R	Remoteness	0.091
WH	Long Working hours	0.091
LK	Lack of Knowledge	0.110
IWD	Improper Work Distribution	0.093
LT	Lack of Time	0.135
S	Snow accumulation	0.640
I	Icing	0.632
MBD	Mains Borne Disturbance	0.600
DRCD	Defective RCD	0.600
MD	Mechanical Damage	0.600
SPL	Supply Power loss	0.600
SBDT	Start-up below the design temperature	0.600
LEC	Loose electrical connections at the contact attachment points	0.600
LCTS	An increase in the load applied to the actuator, i.e. more electrical current across the relay contacts.	0.600

The basic events from A to LT in the above table represent the human factor probabilities. They were estimated by applying the Human Error Assessment and Reduction Technique (HEART), following the guidelines, and using data from Noroozi et al. (2014). Snow accumulation probability was obtained from the snowfall data taken from Pomeroy and Li (2000). Icing probability was estimated as the average probability throughout the year in the Arctic by implying data from Podofillini (2015). For the rest of the basic events (MBD to LCTS), the marginal probabilities were assumed to be 0.6

The BT (Figure 3.6 and 3.7) was mapped into the DBN model (Figure 3.8). For legibility of the BT diagram, the fault tree and event tree constituents are presented separately in Figures 3.6 and 3.7. The fault tree events were transferred as the parent nodes for the "Disruption" node (Table 3.3). The safety barriers were classified as factors contributing to "Adaptation" and "Restoration" capabilities of the separator (Table 3.4). The consequences of BT are presented in Table 3.5. The probabilities presented in Table 3.2 were then inserted in the CPTs of the corresponding root nodes of the DBN.

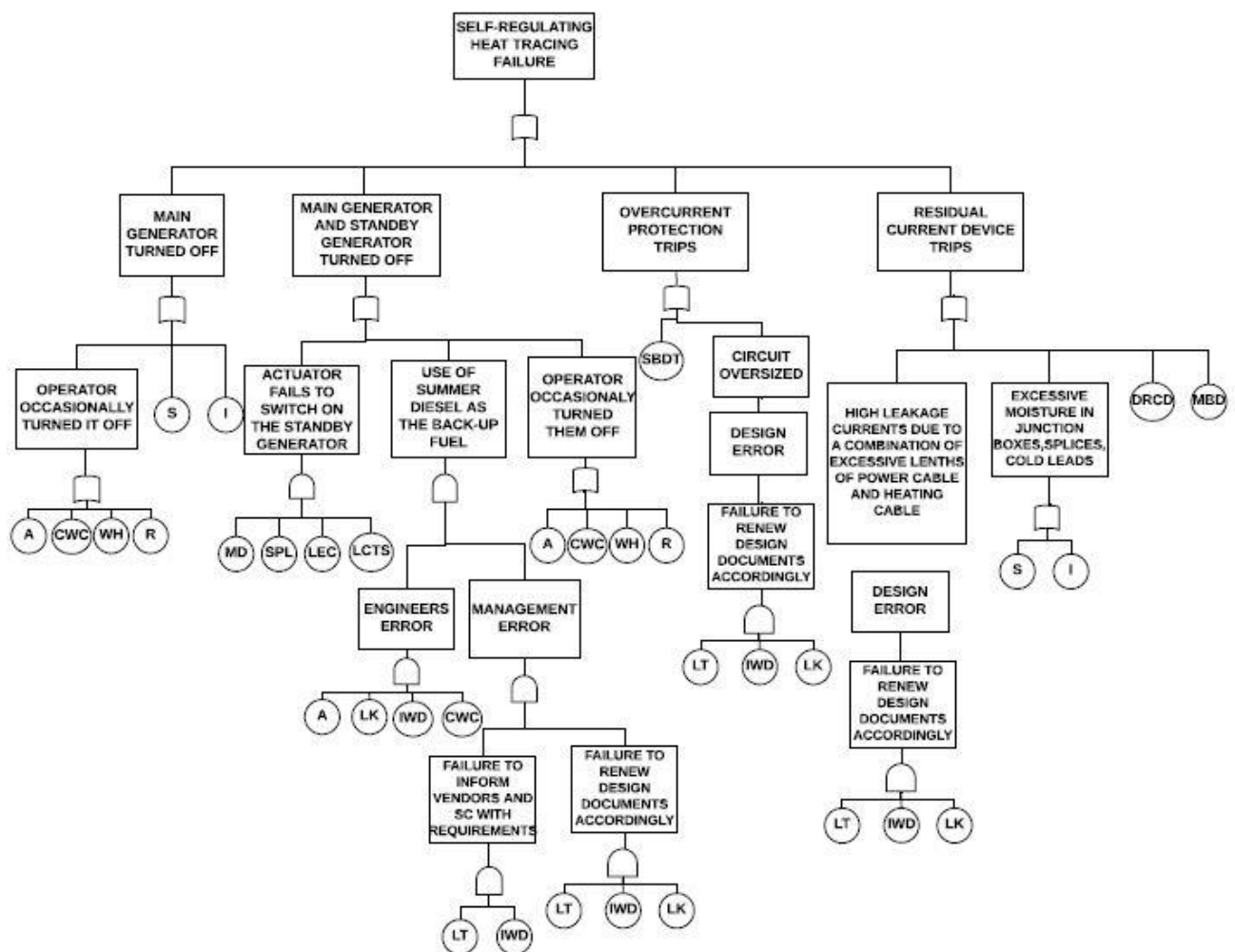


Figure 3.6. The fault tree constituent of the BT diagram

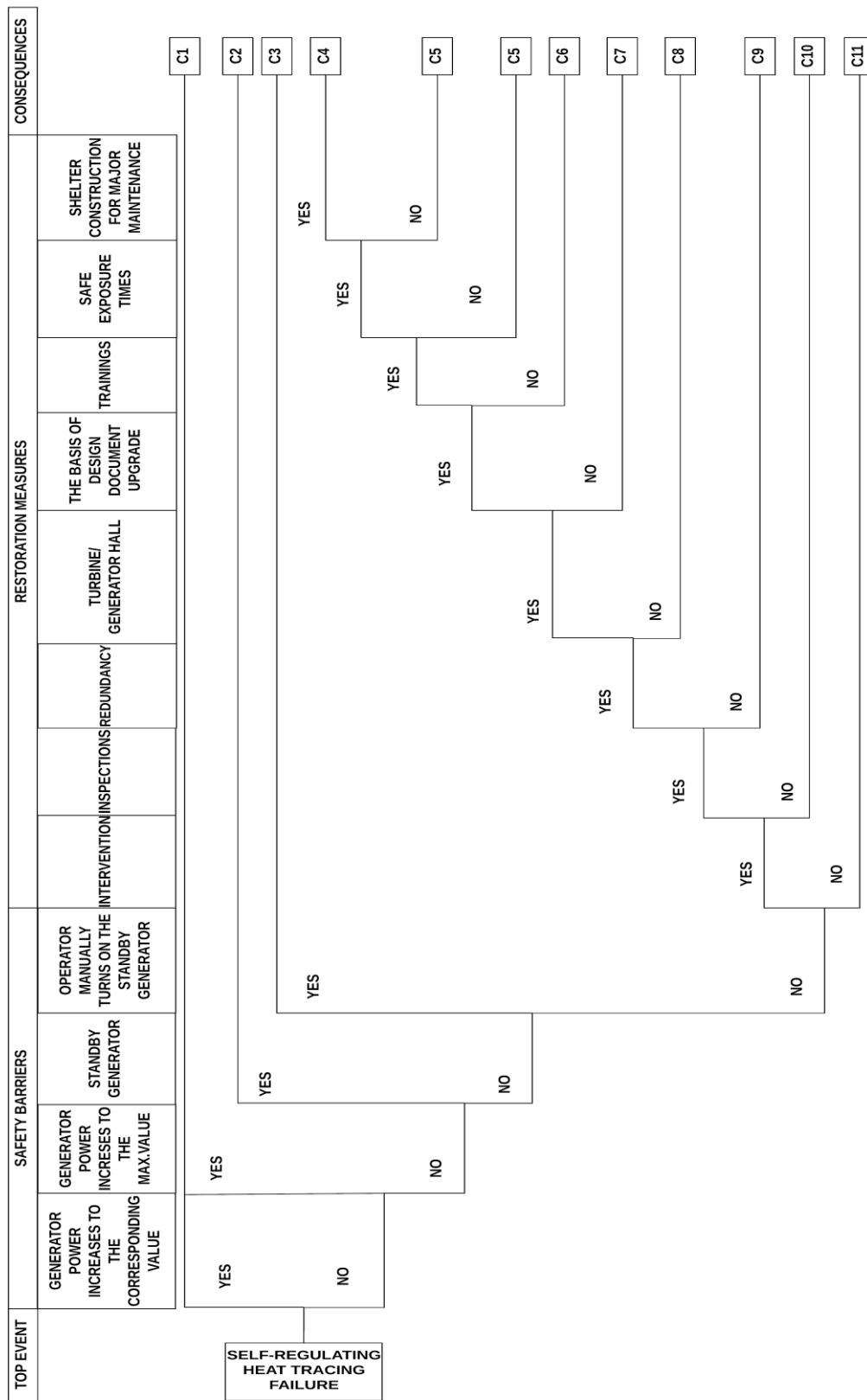


Figure 3.7. The event tree constituent of the BT diagram

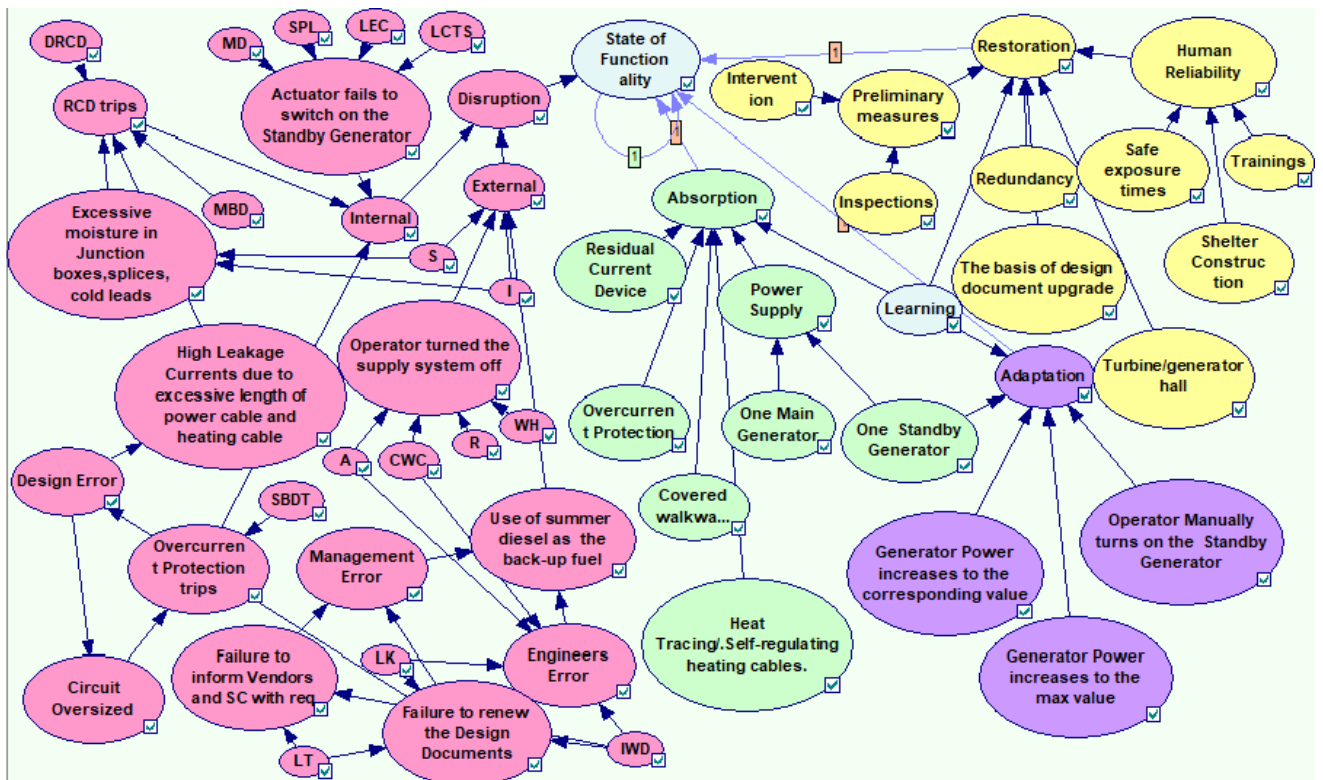


Figure 3.8. The DBN model for resilience assessment (Genie, n.d.)

Table 3.3. External and Internal Disruptions

Disruptions	Parent Nodes
External	The operator turned the supply power off
	Use of summer diesel as the back-up fuel
	Snow Accumulation
	Icing
Internal	Actuator fails to switch on the Standby Generator
	RCD trips
	High Leakage Currents due to excessive length of power cable and heating cable



Table 3.4. The parent and child nodes used for resilience modelling

Child Notes	Parent Nodes
Absorption	Heat Tracing/Self-regulating heating cables
	One main generator
	One standby generator
	Covered walkways
	Residual current device
	Overcurrent protection
Adaptation	Generator Power automatically increases to the corresponding value to compensate the temperature decline
	Generator Power automatically increases to its maximum value
	The standby generator is activated to increase the temperature in separator until the normal operating temperature
	An operator manually turns on Standby Generator if Standby generator is not activated automatically
Restoration	Intervention
	Inspection
	Adding Redundancy: duplicating Main Generators and Stand-By Generators
	Turbine (Generator) Hall Provision with the heaters inside
	Changing the Basis of Design Document, Project Design Philosophies, and Project documentation
	Training to increase the competence level of crew
	Safe exposure times for personnel performing the maintenance(routine) works outside, i.e. 30 min between warm-up breaks in shelters
	Shelter construction for major maintenance works and intricate works with a long duration.

Table 3.5. The classification of consequences in the BT and their association with functionality state

<b>Consequences</b>		<b>Reliability Classification</b>
C1	Loss of main power with imminent reinstatement i.e. short term with no intervention required. Utilities and production are restarted once main power has been re-established.	Medium functionality
C2	Loss of main power with no loss of standby power i.e. standby power is available, all 'essential' i.e. safety and life support systems and 'asset protection' trace heating is available on emergency (standby) power.	Medium functionality
C3	Power reinstatement, monitoring of the system temperature, inspection for the snow accumulation or icing, removal of those with the steam lances	Medium functionality
C4	Fully Resilient system in terms of power availability, human factor minimization, staff knowledge and upgrade of work philosophies based on the results of periodic inspection works	High functionality
C5	System failure may mostly be reasoned by human factor	Low functionality
C6	System failure may mostly be reasoned by human factor and lack of knowledge of personnel	Medium functionality
C7	System failure may mostly be reasoned by the human factor, lack of knowledge of personnel and ignorance to upgrade the documentation based on the results of periodic inspections	Low functionality
C8	System failure probability is high due to the high possibility of the generator being covered with ice or snow as well as due to human factor, lack of knowledge of personnel, and ignorance to upgrade the documentation based on the results of periodic inspections	Low functionality
C9	System failure probability is high due to increased chance of power loss as well as due to human factor, lack of knowledge of personnel, and ignorance to upgrade the documentation based on the results of periodic inspections	Low functionality
C10	The restoration works on the system are not possible without conducting an inspection	Low functionality
C11	The system is not ready for restoration works	Low functionality

### 3.2.2 Resilience assessment using the DBN model

The DBN model of the separator was built, and the dynamic resilience was computed with the GeNIe modeller (n.d.) (Figure 3.8). The DBN model was computed for 100 time-steps with each time step being assumed to be equivalent to one hour of operation. The conditional probabilities for the four states of reliability (S1, S2, S3, and S4) were assigned in the CPT of the "State of Functionality" node applying the data in Tables 3.1 and 4.1 (Yodo et.al., 2017).

Table 3.6. Transition rates for assigning the conditional probabilities of resilience states (Tong and Yang, 2019)

High absorption	$\lambda_1=0.050$
Low absorption	$\lambda_1=0.950$
High adaptation	$\mu_1=0.150$
Low adaptation	$\mu_1=0.000$
High restoration	$\mu_2=0.250$
Low restoration	$\mu_2=0.000$
Reliability degradation	$\lambda_2=0.001$

Figure 3.9 presents the dynamic probability profile of the four different functionality states of the system. S1 starts from the time when the disruption occurs (the system having a high functionality state at time  $t=0$ ). S1-S2 region (from  $t=0$  till the intersection of the S1 curve with the S2 curve) shows the region where the state of the system functionality decreases because the absorption capability of the system was not high enough, disruption occurred at 8 hours, after the adaptation (S2-S3) has started. S2-S3 region is the region from the intersection of S1 and S2 curves till the intersection of S1 and S3 curves. S3-S4 region starts from the intersection of S1 and S3 curves and continues up till the end of S4 curve. As can be seen, at 20 hours, the adaptation curve reaches its peak and then decreases for letting the restoration (S3-S4) take place, bringing the system to the new state of S4. After 60 hours, the probabilities of all the four functionality states are stabilized. The newly achieved probability of functionality of the separator after the restoration is  $S4=97.73\%$ .

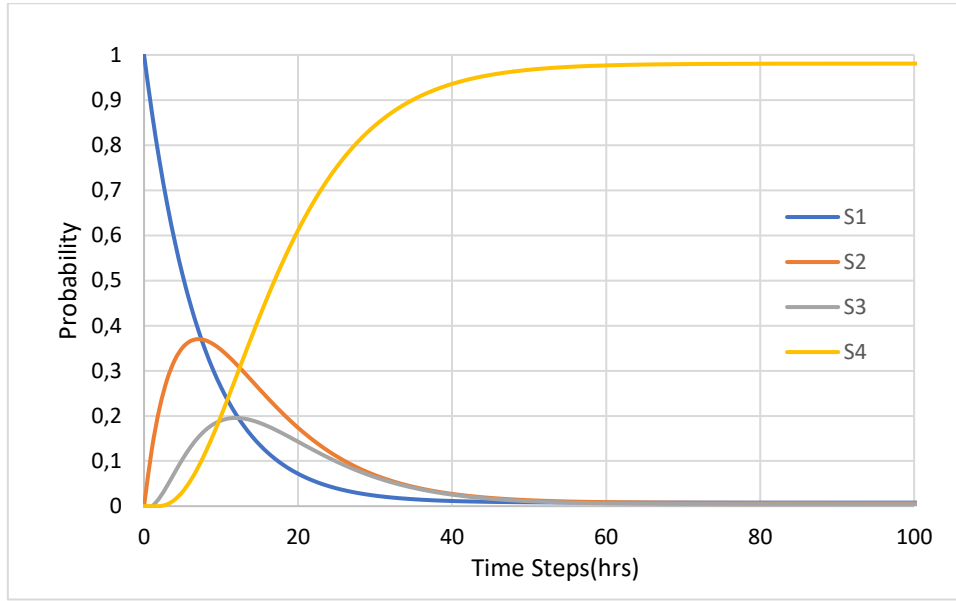


Figure 3.9. The dynamic probability profile of four functionality states

Figure 3.10 shows the resilience profile of the separator. The profile is obtained by summing the probabilities of the initial state of functionality, S1, and the recovered state of the system, S4. It could be seen that the resilience of the system changes with time until it stabilizes at about 60 hours with a new resilience of 98.48 %. The rapid decline of the resilience at 9 hours is associated with the disruption due to the heat tracing failure, and a further increase of the resilience from that stage is due to the system's adaptation and external restoration attempts. The learning capability of the system during this process of disruption occurrence would contribute to an increase in absorption, adaptation, and restoration capabilities. This would consequently facilitate the achievement of higher levels of system resilience.

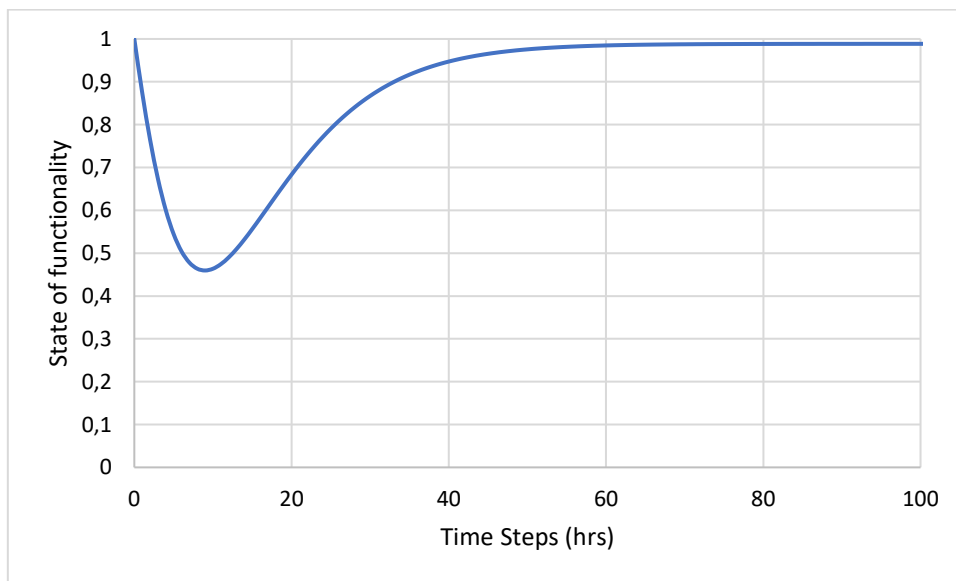


Figure 3.10. The dynamic change of the separator's resilience

### 3.2.3 Design for a more resilient system

With the purpose to validate the model, the posterior analysis was conducted using the DBN model. Additional nodes (shown in Table 3.7) were placed as parent nodes for "Absorption", "Adaptation" and "Restoration". A new DBN model (Figure 3.11) was developed.

The system has already undergone the disruption and learning process throughout its recovery. The joint probabilities of "State of Functionality" in 100 hours were re-estimated by GeNIe (n.d.). The addition of safety measures facilitates the enhancement of the system's resilience. Therefore, the separator resilience obtained at this stage should be higher than the previous one.

Table 3.7. Additional parameters

Absorption	Anti-freeze additives or use of low-temperature fluids in liquid systems
	Wind barriers for equipment (exacerbating snow accumulation too)
Adaptation	Automated steam lances are used for ice removal from the separator and auxiliary equipment
	Independent temperature limitation devices. An additional, independent temperature limiter ensures that if the control thermostat fails, the surface temperature of the heating cable will not exceed the maximum allowed temperature for the hazardous area by switching off the heating cable.
Restoration	Size overcurrent protective devices according to the design specification and/or local standard practices. This means to accurately select the ampere, voltage and interrupting ratings for overcurrent protective devices based on the design specification and/or local standard practices.

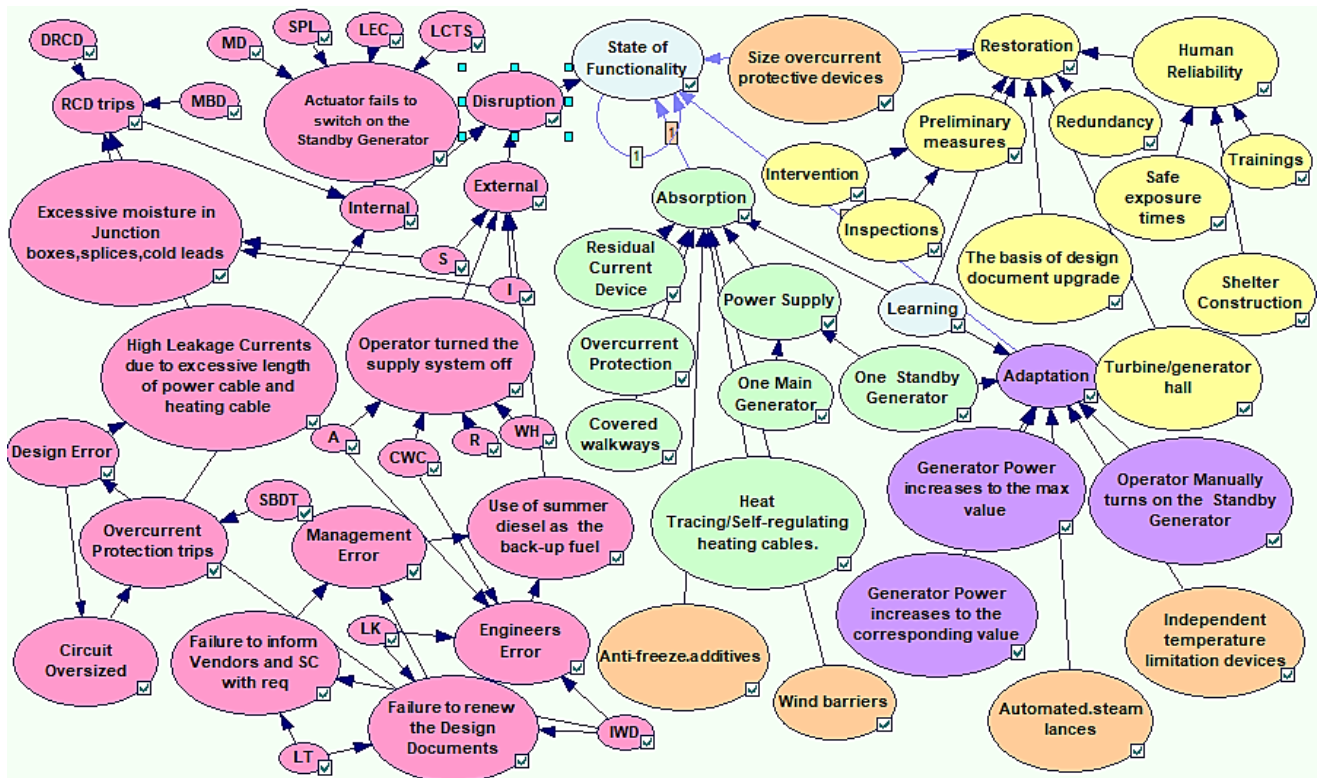


Figure 3.11. The new DBN model (with additional nodes) for resilience assessment of a separator (Genie, n.d.)

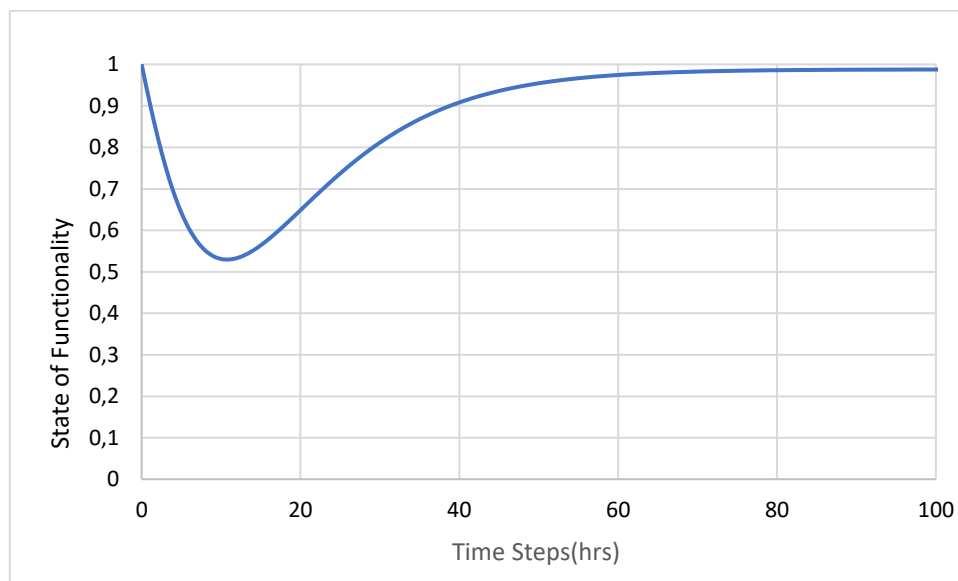


Figure 3.12. The resilience of the separator with new design

Table 3.8. Comparison of resilience metrics

<b>Resilience metrics</b>	<b>DBN Model 1 (Figure 3.10)</b>	<b>DBN Model 2 (Figure 3.12)</b>
Disruption occurrence time (hrs)	9	11
Resilience decline value (%)	46%	53%
The probability of the final resilient state S4 (%)	98.48%	98.27%
Time for resilience stabilization (hrs)	60	70
Time for 90 % recovery (hrs)	34	40

From Figure 3.12 and Table 3.8 it could be seen that disruption has occurred at 11 hours, indicating a higher absorption for the refined DBN model. The resilience declined to 53%, which is 7% higher than that of the previous model. The final resilient state S4 is presumably the same  $S4 = 98.27\%$  as obtained in Section 3.2.2. However, it takes a longer time for the resilience to stabilize, i.e.,  $t_4 = 70$  hrs. This is because the added parameters (operations) have their own operational time that contributes to the longer duration of the resilience stabilization. These results partially validate the DBN model for resilience assessment as the predicted resilience increased as the additional arrangement was made to improve the system's adaption. Having the resilience dynamics helps to determine the extent to which the disruption may affect the system functionality and how long it takes (depending on the time-step amount) to recover the system to the normal operational state with the addition of resilience measures.

For normal operation, we assume that at least 90% of its original resilience needs to be achieved. 90% probability of recovery to the high functionality state is obtained as shown in Figure 3.12 at about 40 hours, which is longer than the previous case due to the additional hours of the newly added stabilizing operations in Figure 3.10.

### 3.2.4 Posterior analysis

For posterior analysis, four nodes were selected, “Snow”, “Icing”, “Power Supply” and “Safe Exposure Times”. For each of them, pieces of evidence were recorded for 10-time steps (Table 3.9). The “Yes” evidence in Table 3.9 designates a 100% probability of occurrence of each event in the node. The given analysis is conducted for observing how the separator will restore in case of the continuous snowfall, icing formation above the equipment, loss of one of the power supply units and increased human factor due to the long period of work in the cold. As a result, the resilience curve in Figure 3.13 is obtained.

Table 3.9. Pieces of evidence for selected nodes

Node designation	Meaning	State
S	Probability of heavy snowfall	High
I	Probability of serious icing on the unit and auxiliary equipment	High
Power Supply	Either Main Generator or Standby Generator not working	Yes
Safe exposure times	Maintenance and routine works are conducted outside for more than the set safe exposure time (i.e. 30 minutes)	Yes

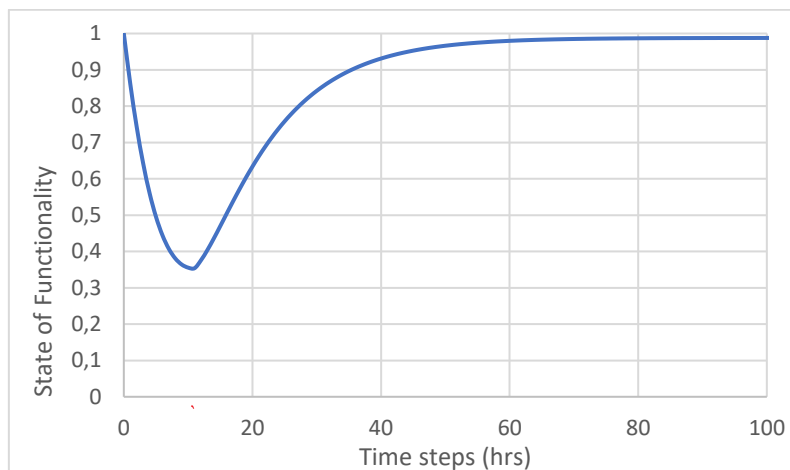


Figure 3.13. The resilience profile obtained as a result of the posterior analysis.



Table 3.10. Comparison of prior and posterior Resilience parameters

Resilience metrics	Prior analysis (Figure 3.10)	Posterior analysis (Figure 3.13)
Disruption occurrence time (hours)	9	11
Resilience lowest value (%)	46%	35%
Final resilient state S4 (%)	98.48%	98.52%
Time for resilience stabilization (hrs)	60	70
Time for 90% recovery(hrs)	34	36

Table 3.10 presents the comparison between the prior (Figure 3.10) and posterior (Figure 3.13) resilience analysis results. Even though the disruption effect was higher with the malfunction of the power supply system, the increase of human factor, and the harsh environmental conditions, the separator with the advanced resilience attributes was able to restore to its normal operational state (98.52%). However, the damage to the reliability of the system was higher, with the reliability reducing to 35% and with more extended time for the system to restore (70 hours).

### 3.2.5 Sensitivity analysis

The sensitivity analysis was conducted to identify the critical parameters contributing to the variation of the system resilience. First, the node “State of Functionality” was selected as the target node for sensitivity analysis. Then each of the parameters was sequentially changed to the low operational state and high error probability state. Table 3.11 presents all these scenarios. The dynamic resilience curve was obtained for each scenario, and the summary of the results was presented in Table 3.12. The most significant reduction of the system’s resilience occurs when the state of absorption is low. This designates the weak inherent safety design of the system. The most significant effect resulting in the drop of the absorption occurs due to malfunction of the Residual Current Device, Overcurrent Protection and the Standby Generator. The proper adaptation and restoration parameters facilitate the restoration of the system in the short amount of time compared with the change in the other nodes (Table 3.12). The parameters that contribute to a shorter time of resilience recovery are adaptation parameters, such as the generator power increases to the corresponding and maximum value in response to the temperature drop, and the standby generator activation. As for the restoration parameters, the most effect on the fast resilience recovery is due to the factors such as redundancy of the power

supply equipment, the upgrade of the basis of design document, the increase of the human reliability factors due to shelter construction for maintenance works, safe exposure times and trainings for the operating personnel. For scenarios 5, 6, and 7 the system shows the least change of the resilience due to the well-thought safety design, responding to restore the system to the normal operational state.

Table 3.11. The scenarios used for sensitivity analysis

<b>Scenario 1</b>	The standby generator was not switched on
<b>Scenario 2</b>	Low Human reliability
<b>Scenario 3</b>	Safe exposure time is more than 30 minutes
<b>Scenario 4</b>	Low Restoration
<b>Scenario 5</b>	High level of Disruption
<b>Scenario 6</b>	High error probability of Overcurrent protection
<b>Scenario 7</b>	High error probability that RCD Trips
<b>Scenario 8</b>	Generator power does not increase to the corresponding value
<b>Scenario 9</b>	Low Absorption
<b>Scenario 10</b>	Low Adaptation

Table 3.12. The results of the Sensitivity Analysis

<b>Scenarios</b>	<b>Resilience reduction (%)</b>	<b>Time to reach lowest reliability(hrs)</b>	<b>Time to 90 % recovery (hrs)</b>
1	28.89	17	41
2	44.98	13	39
3	51.71	11	39
4	21.78	16	40
5	52.47	11	39
6	52.94	11	39
7	52.93	11	40
8	50	12	40
9	0.25	2	23
10	16.87	17	43

Overall, the case study demonstrated the effectiveness of integration of BT and DBN for dynamic quantitative resilience assessment for the specific accident scenarios development.

# Chapter 4- Dynamic QRA of separator at standard ambient conditions: Integration of FRAM and DBN approach

## 4.1 The proposed methodology for dynamic resilience assessment with FRAM and DBN integration

*A version of this chapter has been submitted to the **Journal of Reliability Engineering and System Safety**. I am the primary author. Co-author Ming Yang provided much needed support in implementing the concept and testing the model. I have carried out most of the data collection and analysis. I have prepared the first draft of the manuscript and subsequently revised the manuscript, based on the feedback from Co-authors. The three Co-authors assisted in developing the concept and testing the model, reviewed and corrected the model and results. They also contributed in reviewing and revising the manuscript.*

Figure 4.1 describes the methodology employed in this study. First, the FRAM analysis of the process system will be accomplished in conjunction with the Monte Carlo Simulation. Resultantly, the critical coupling will be identified. For the critical coupling, the attributes of the resilience will be developed, and the DBN model will be built. The conditional probability tables of the nodes in DBN will be filled with probabilities of failures (POF) collected from literature, prescribed by Subject Matter Experts(SMEs), and calculated with the Aspen Hysys simulation.

Afterwards the resilience curve will be generated with the Genie Simulation. Next, the DBN model will be updated with additional safety measures, and the generated resilience curve will be compared with the previous resilience profile. After that, the first developed DBN model will undergo sensitivity analysis for the identification of the most important safety measures. Finally, the developed resilience model will be reassessed for worn-out equipment conditions.

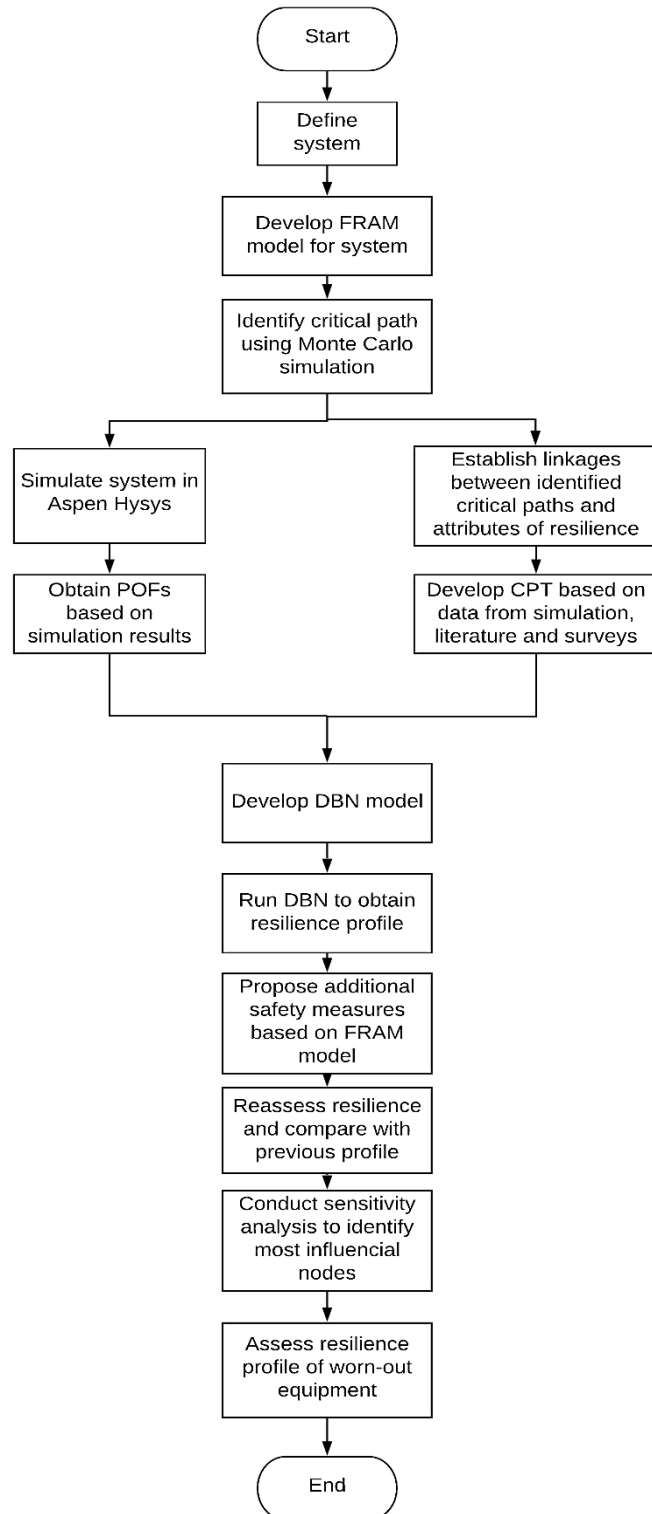


Figure 4.1. The proposed methodology for dynamic resilience assessment

#### **4.1.1 Development of the FRAM model**

Functional Resonance Analysis Method (FRAM) model consists of the main activities done by or on the complex system and enables identification of the root causes of the accident on the level of the socio-technical interactions. This is a new approach in the sphere of the safety analysis, conforming to the perspectives of Safety-II, which states that the causes of the accidents may be identified on the level of socio-technical aspects interaction in a transient manner (Hollnagel, 2012).

At the beginning of the FRAM analysis, it is necessary to identify the goal of the FRAM analysis, specifically whether it is accident investigation analysis or the risk assessment (Rosa et al., 2015). The development of FRAM consists of four steps, mainly:

##### *Step 1: Identifying and describing the functions of the system*

Firstly the main activities or functions performed by or on the system to reach a specific outcome every day are defined. Functions are interconnected via the aspects placed in the corners of the hexagon according to the Structured Analysis and Design Technique (SADT). Each function consists of the six aspects, namely input, output, precondition, resources, time, and control. The function output of which serves as one of the other five aspects for the other function in the coupling is named as upstream function; the other joint function is named as the downstream function. The following gives the six aspects of a function.

- Input (I)- the aspect that initiates the function
- Output (O)- the outcome of the function, serves as the input for the downstream function
- The precondition (P)- the condition that should be performed before the initiation of the downstream function
- Resource (R)- what the function needs to produce the output
- Time (T)- temporal requirements or constraints obliged to the function, such as start time or finish time.
- Control (C)- what performs the control and monitoring of the function to achieve the set outcome (Tian, 2016)

### *Step 2: Identifying the variability of the system*

Each function has its variability. Variability could be classified as positive if it reduces the risk of possible accident development or negative if it facilitates the accident development scenario. According to Hollangel (2012), variability could be classified based on multiple phenotypes, such as time, precision, flow rate, speed, duration, direction, object, force. In this study, variability manifestation based on time and precision will be used. The reasons are a) the user-friendly readability of the analysis, and b) the universal application of those phenotypes for any function.

Based on time, the variabilities are classified as on time, too late, too early, and not at all. Not at all is used for the cases when the function is performed that late, that the outcomes of it are of no longer point of interest to consider. Based on precision, the variabilities are classified as precise, acceptable, imprecise, and wrong. Based on the SME's judgment those classifications are ranked with numbers and further used in Monte Carlo Analysis (Patriarca et al., 2017).

### *Step 3: Aggregating the variabilities*

This step deals with the variability of the couplings. Variability of the couplings may arise as a result of each function's inner variabilities or as a result of the impact of the upstream function. In case when the coupling produces the large negative variability, this consequently results in the resonance of the connected functions and identifies the critical path. The critical path defines the leading cause of the accident in the accident investigation scenario, or the main factors contributing to the hazard development in risk assessment.

If the upstream function generates positive variability, this results in the dampening of the variability of the downstream function (Patriarca et al., 2017).

In this study in step 3, the Monte Carlo Simulation is integrated to identify the exact critical path resulting in the malfunction of the two-phase separator of the acid gas sweetening unit.

### *Step 4: Managing the variability and suggesting the solutions to identified critical path*

Step 4 monitors the variabilities of the performance. The purpose of step 4 is to suggest measures to increase positive variabilities and decrease negative variabilities. The recommendations are suggested for the identified critical path to avoid the accident from happening, or in case of an accident happened to restore the system to the high functional state.

As the continuation of step 3, for the critical path identified, we develop the DBN model recommending the absorption, adaptation, and restoration parameters to either absorb the possible disruption or to recover from it.

#### ***4.1.2 Monte Carlo analysis for identification of the critical path***

Monte Carlo Simulation (MCS) is the tool for the mathematical calculations for complex systems using random sampling for adhering the outcomes close to reality (Zio, 2013). In this research work, the MCS is used for the estimation of cumulative variabilities in the FRAM model. The idea of Monte Carlo application for the estimation of the cumulative variability in the FRAM Model was taken from the work of Patriarca et al. (2017). In their work, they identified the critical couplings having the highest risk of causing an accident. They also provided the resonant path that emerges because of the variability accumulation for the neighboring functions to the critical couplings. The critical couplings were determined at step 4 of the FRAM analysis by setting the critical cumulative variability value and the confidence level of 95 %. The couplings for which 5% of the cumulative variabilities generated with the Monte Carlo simulation were higher than the setpoint value, equal to 24, were classified as critical. Hence, the corresponding recommendations were provided to avoid the accident occurrence.

In this research paper, a similar approach of MCS for cumulative variability estimation is employed for the identification of the critical couplings in FRAM. However, MCS in this research paper also serves as a function of the logical bridge between the FRAM Model and the DBN model for the quantitative resilience assessment of the process unit.

##### ***Step 1. Defining the probabilities***

From the SMEs judgment in the work of Patriarca et al. (2017), the discrete probability distributions for each of the four variability states based on the timing and precision were defined (Tables 4.1 to 4.3).

Table 4.1. Variability scoring based on Timing and Precision

	Variability	Score
Timing	On-Time	1
	Too Early	2
	Too Late	3
	Not at all	4
Precision	Precise	1
	Acceptable	2
	Imprecise	3
	Wrong	4

Table 4.2. Discrete Probabilities Distributions for Timing variabilities

	1	2	3	4
Probability of being too early	0.15	0.7	0.1	0.05
Probability of being on-time	0.7	0.15	0.1	0.05
Probability of being too late	0.15	0.05	0.7	0.1
Probability of not at all	0.1	0.05	0.15	0.7

Table 4.3. Discrete Probabilities Distributions for Precision variabilities

	1	2	3	4
Probability of being Precise	0.7	0.2	0.05	0.05
Probability of being Acceptable	0.05	0.7	0.2	0.05
Probability of being Imprecise	0.05	0.2	0.7	0.05
Probability of being Wrong	0.1	0.1	0.1	0.7

*Step 2. Assigning the amplification factors for each coupling*

The amplification factors are also distributed based on the timing ( $\alpha_{ij}^T$ ) and precision( $\alpha_{ij}^P$ ) relations of the upstream and downstream couplings. Based on the effect of the variability of the upstream function conveyed to the downstream functions, the amplification for both timing and precision are assumed in the following ranges:



Table 4.4. The ranges for amplification factors (Patriarca et al,2017)

$\alpha_{ij}^T (or \alpha_{ij}^P)$	
$>1$	If the variability of the downstream function is amplified by the output of the upstream function
$=1$	If the variability of the downstream function is not affected by the output of the upstream function
$<1$	If the variability of the downstream function is dampened by the output of the upstream function

### Step 3 Calculation of the OV and CV

Overall variability is the multiplication of the variabilities of upstream functions based on timing ( $V_j^T$ ) and precision ( $V_j^P$ ) (4.1)

$$OV_j = V_j^T * V_j^P \quad (4.1)$$

The cumulative variability ( $CV_{ij}$ ) is the joint variability of the coupling. It is estimated by multiplication of the overall variability and amplification factors for timing and precision assigned for the corresponding coupling.

$$CV_{ij} = OV_j * \alpha_{ij}^T * \alpha_{ij}^P \quad (4.2)$$

In MCS the normal distribution equation is applied for the variability ranges based on timing and precision (Tables 4.1 and 4.2), amplification factors range assigned by SMEs (Patriarca et.al, 2017). Resultantly, 1000 random numbers are generated with MCS for the cumulative variabilities of each of the function couplings (4.2).

### Step 4 Identification of critical path

At the next stage, the setpoint and the confidence level are assigned. The confidence level in this work is set to be equal to 95 %. Hence, after the generation of 1000 random numbers, five percentiles of them is compared with the set point. In case if the five-percentile number is higher than the setpoint, the corresponding coupling is set as the critical one. The further recommendations and the work on risk prevention or accident recovery are prioritized, starting from the coupling with the highest five percentile number.

#### ***4.1.3 Preliminary development of the DBN model based on the most critical coupling***

The “Absorption”, “Adaptation”, and “Restoration” nodes are complemented with the nodes corresponding to the most critical coupling obtained as a result of the FRAM and MCS. For example, the case study described below identifies the most critical coupling as the level controllers and interlock system inaccurate performance and late or inaccurate response of the operator in the control room. Thus, the nodes for “Absorption”, “Adaptation” and “Restoration” were selected corresponding to only the performance of the level controllers and the interlock system and the performance of the operator in the control room.

- (1) Building the DBN model based on the Absorption, Adaptation, Restoration and, Learning parameters for the most hazardous case identified with the FRAM model.
- (2) Filling the conditional probability tables (CPT) of the nodes with the help of simulations, historical data, and data from the surveys.
- (3) Getting the resilience curve as the summation of the initial state of the system (S1) and its restored state (S4).

#### ***4.1.4 Application of simulation to the extraction of POFs***

The POFs are extracted from Aspen Hysys Dynamics simulation for acid gas sweetening unit using the strip charts for the parameters characterizing the performance of the process system of interest (Hysys,2004). From the strip chart, the time range of the system malfunction or being in the out of normal operating range is divided by the total time range of operations (4.3).

$$POF = \frac{\text{Malfunction time range}}{\text{Total operational time}} \quad (4.3)$$

The POF characterizing the functioning of the process system could also be extracted from Aspen Hysys Sensitivity analysis. For this case simulation is run at the specified range of the several input parameters. As a result of the analysis for 1000 iterations, the output is monitored for the number of scenarios out of the normal range scope. Then, the POF is estimated as the ratio of the amount of the abnormal outcomes to the total number of outcomes (4.4).

$$POF = \frac{\text{No .of abnormal outcomes}}{\text{Total no.of outcomes}} \quad (4.4)$$

The estimated POFs are then inserted into the corresponding nodes of the DBN model and the resilience curve is derived.

#### ***4.1.5 Reassessment of the Resilience Curve with the inclusion of additional safety measures in the DBN model***

For "Absorption", "Adaptation" and "Restoration" nodes additional safety nodes are added. Then the resilience profile is compared with the previous resilience curve. The updated resilience model should present the enhanced resilience properties for a long time until the functionality drops and the higher value of the functionality is attained after the restoration stage.

#### ***4.1.6 Sensitivity Analysis for identification of the most influential nodes***

Sensitivity analysis facilitates the identification of the nodes having the highest impact on the state of the system's functionality. This will assist in the application of the specific safety measures for the system.

#### ***4.1.7 The assessment of the resilience profile of worn-out equipment***

To assess the evolution of the resilience with time at the case of the equipment being worn-out due to corrosion, the outcomes of the research done by Liao et.al. (2011) will be used. In that research, the Weibull distribution equation was employed for the Reliability estimation (4.5)

$$R(t) = \exp \left[ - \left( \frac{t}{\eta} \right)^\beta \right] \quad (4.5)$$

, where R(t)- reliability value after a certain time t,  $\beta$ - shape parameter and  $\eta$ - scale parameter.

The parameters were estimated with the employment of least-squares parameter estimation and mean rank method. In the work of Liao et.al. (2011) the reliability estimation was performed for engine after 2,000 hours of operations. It was assumed that the separator was made from the same material. The estimated reliability of 70.36% was multiplied for previously developed probabilities of success. The probabilities of failure were also calculated accordingly. Consequently, the resilience profile for the worn-out equipment was achieved with the employment of Genie simulation.

## 4.2 Case Study 2

were generated accordingly for 1000 outputs of cumulative variability. Setting the 95% confidence level, and setpoint value of 24 for overall variability, the outcome of each of 31 couplings was compared with the setpoint value. If the 5-percentile value of the given coupling was greater than 24, it was considered as critical (Figure 4.3). In the following case, the coupling of the highest criticality was considered, which is the coupling of the Operator of the control room controlling the level and interlock system, resulting in the cumulative variability value at 5 percentiles of 38. Thus, imprecise and/or too late a response of the operator at the control room to the level alarms and indicators has the highest potential to cause an accident. Furthermore, the imprecise performance or too late a response of the level alarm and interlock systems has the highest potential to result in the accident or two-phase separator failure.

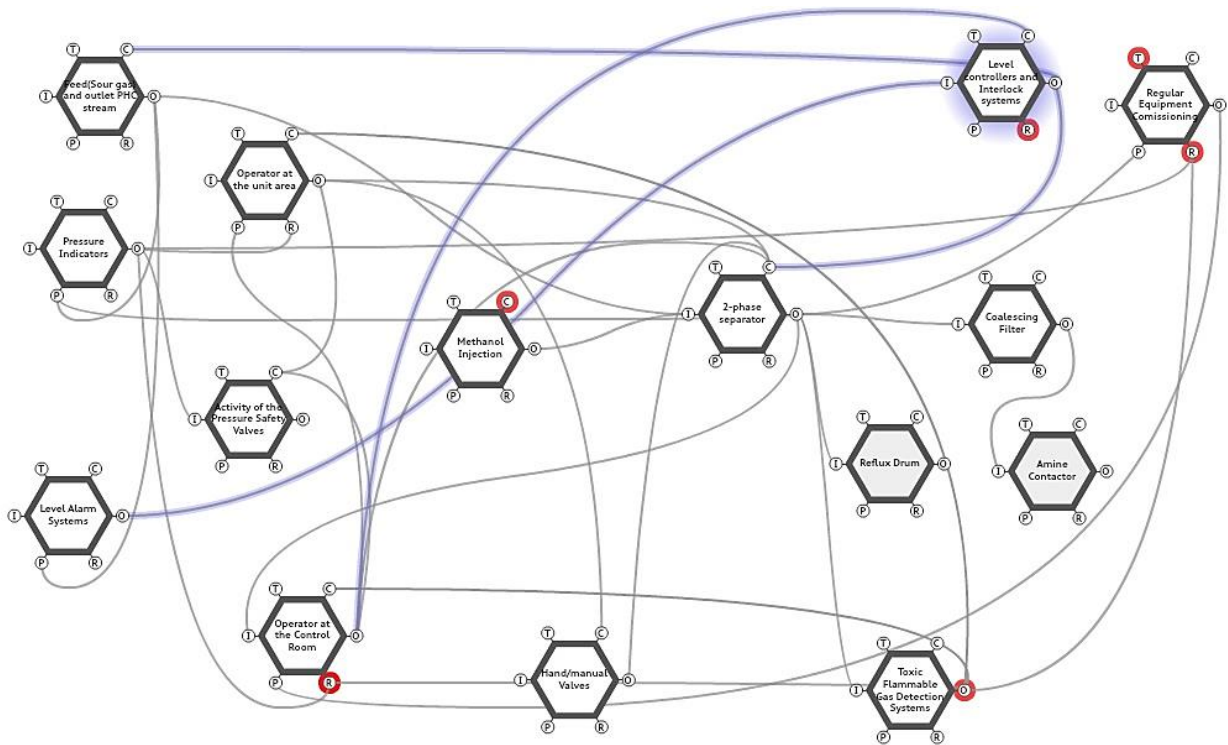


Figure 4.3. FRAM Model for the activities related to the 2-phase separator

Table 4.5. The FRAM couplings with indicated amplification factors.

Downstream function		Upstream function				
Name of function	Aspect	Name of function	$\alpha_{Tij}$	$\alpha_{Pij}$	Couplings	5%
2-phase separator	Input	Feed(Sour gas + PHC)	10 $\pm$ 3	40 $\pm$ 20	C1	1.21
	Input	Methanol Injection	30 $\pm$ 20	30 $\pm$ 20	C2	0.00
	Control	Operator at the Control Room	50 $\pm$ 20	40 $\pm$ 20	C3	3.62
	Control	Operator at the unit area	50 $\pm$ 20	50 $\pm$ 20	C4	7.40
	Control	Level controllers and Interlock systems	60 $\pm$ 20	50 $\pm$ 10	C5	18.70
	Control	Hand/manual Valves	10 $\pm$ 5	10 $\pm$ 5	C6	0.06
Feed(Sour gas + PHC)	Control	Level controllers and Interlock systems	60 $\pm$ 30	40 $\pm$ 20	C7	2.42
Pressure Indicators	Precondition	Feed(Sour gas + PHC)	10 $\pm$ 5	10 $\pm$ 5	C8	0.12
	Precondition	2-phase separator	10 $\pm$ 6	10 $\pm$ 6	C9	0.01
Pressure Safety Valves	Input	Pressure Indicators	60 $\pm$ 10	40 $\pm$ 10	C10	17.84
	Control	Operator at the Control Room	70 $\pm$ 10	50 $\pm$ 10	C11	26.90
	Control	Operator at the unit area	60 $\pm$ 20	50 $\pm$ 20	C12	12.88
Level Alarm Systems	Precondition	Feed(Sour gas + PHC)	10 $\pm$ 7	10 $\pm$ 7	C13	0.00
Level controllers and Interlock systems	Input	Level Alarm Systems	80 $\pm$ 10	50 $\pm$ 20	C14	23.67
	Control	Operator at the Control Room	70 $\pm$ 20	80 $\pm$ 10	C15	37.88
Toxic Flammable Gas Detection Systems	Precondition	2-phase separator	10 $\pm$ 3	10 $\pm$ 3	C16	0.52
Operator at the Control Room	Precondition	Regular Equipment Commissioning	40 $\pm$ 30	50 $\pm$ 30	C17	0.01
	Resource	Toxic Flammable Gas Detection Systems	50 $\pm$ 20	60 $\pm$ 20	C18	11.89
	Resource	Pressure Indicators	50 $\pm$ 20	60 $\pm$ 30	C19	4.93
	Resource	2-phase separator	10 $\pm$ 2	10 $\pm$ 2	C20	0.73
	Control	Toxic Flammable Gas Detection Systems	40 $\pm$ 20	50 $\pm$ 20	C21	3.57
Operator at the unit area	Resource	Pressure Indicators	10 $\pm$ 3	60 $\pm$ 20	C22	3.19
	Control	Toxic Flammable Gas Detection Systems	70 $\pm$ 10	60 $\pm$ 20	C23	26.03
	Precondition	2-phase separator	10 $\pm$ 1	70 $\pm$ 10	C24	5.96
Regular Equipment Commissioning	Resource	Toxic Flammable Gas Detection Systems	10 $\pm$ 6	50 $\pm$ 30	C25	0.01
	Resource	Pressure Indicators	10 $\pm$ 7	60 $\pm$ 30	C26	0.02
	Time	Operator at the unit area	50 $\pm$ 30	60 $\pm$ 20	C27	0.88
Coalescing Filter	Input	2-phase separator	10 $\pm$ 1	20 $\pm$ 10	C28	0.74
Amine Contactor	Input	2-phase separator	10 $\pm$ 3	30 $\pm$ 20	C29	0.01
Reflux Drum	Input	2-phase separator	30 $\pm$ 10	40 $\pm$ 10	C30	7.02
Hand/manual Valves	Control	Operator at the unit area	50 $\pm$ 30	60 $\pm$ 20	C31	0.06

#### 4.2.2 DBN Model

Based on the outcome of the FRAM analysis, the DBN Model is developed for the coupling with the highest criticality (Figure 4.4). The node "Disruption" lists the potential malfunctions that may cause accident development. The nodes "Absorption" and "Adaptation" list the current safety absorption and adaptation measures applied for the two-phase separator. "Restoration node" includes the recommendations for the enhancement of the 2-phase separator performance.

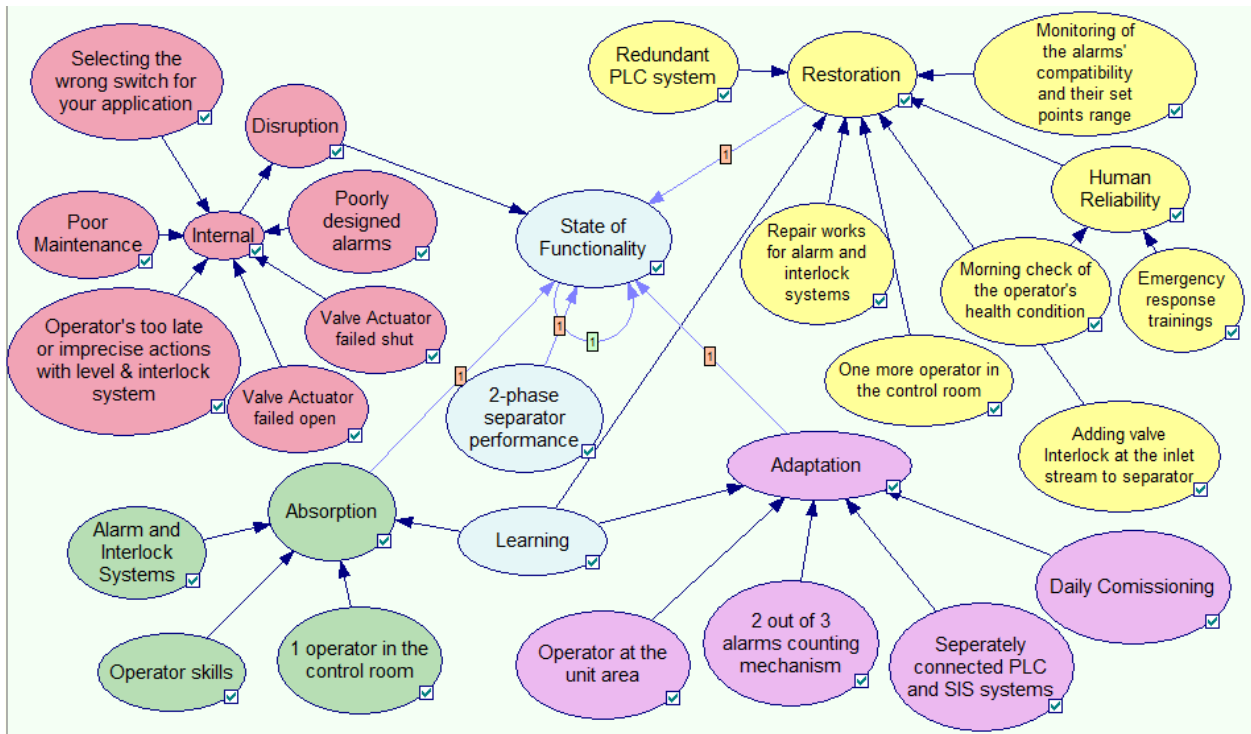


Figure 4.4. Developed DBN model for the identified critical path

#### 4.2.3 Application of simulation for extraction of POFs

The probability of failure for “2-phase separator performance” node was measured with sensitivity analysis in the Aspen Hysys model (Figure 4.2) with 700 iterations. The input parameters were the ranges of the pressure, temperature, and flow rate of the feed. The output parameter was the dihydrogen sulfide concentration in the "Sweet Gas" stream, leaving the amine contactor. As the failure, the case of having the  $H_2S$  concentration higher than 4 ppm was assumed. Consequently, the POF equivalent to 0.122 was estimated.

The POFs of the other nodes were identified using Aspen Hysys Dynamic simulation scenarios (Figure 4.5).

##### *Scenario 1. Valve actuator Failed Open.*

The Aspen Hysys Dynamic simulation for estimation of POF was completed for the two-phase separator located before the absorption column (Figure 4.2). The products of the separator were the sour gas routing to the absorption column and process hydrocarbons routing to the stabilization unit. The POF evaluation was accomplished with the strip charts generated as a result of the dynamic simulation (Figure 4.6). For filling the disruption node "Valve actuator Failed Open", the valve VLV-102 fail-open scenario was simulated in Aspen Hysys

Dynamic(Figure 4.5). The normal liquid per cent level was set to the value of 20-50%, however, the level of liquid in the tank dropped to 4.13 % when the valve VLV-102 failed open(Figure 4.2). Employing Eq. (4.3) the POF for the node “Valve actuator failed Open” was estimated :

$$POF_1 = \frac{\text{Malfunction time range}}{\text{total operational time}} = \frac{56540 \text{ min} - 56301 \text{ min}}{56540 \text{ min} - 55340 \text{ min}} = \frac{239 \text{ min}}{1200 \text{ min}} = 0.199$$

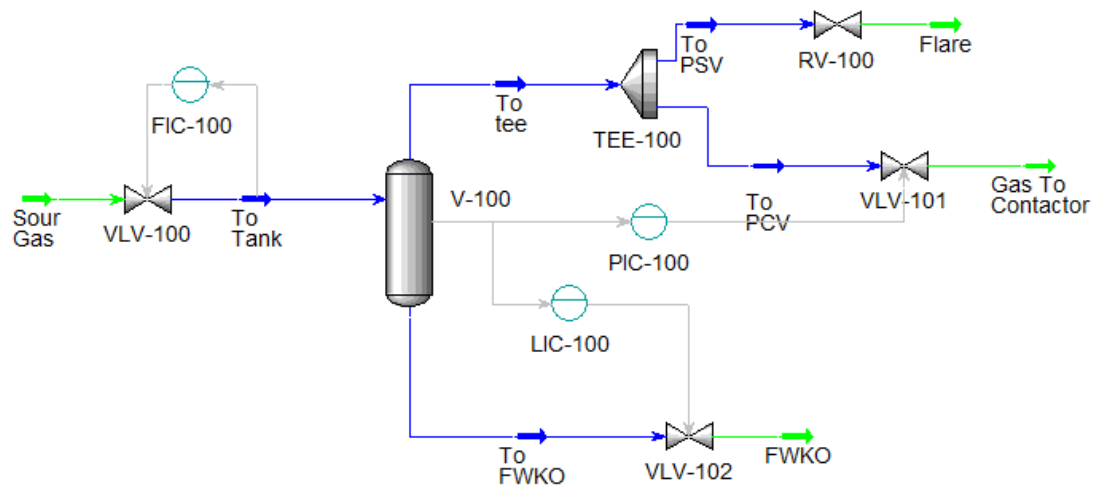


Figure 4.5. Process control of the 2-phase separator(Hysys,2004)

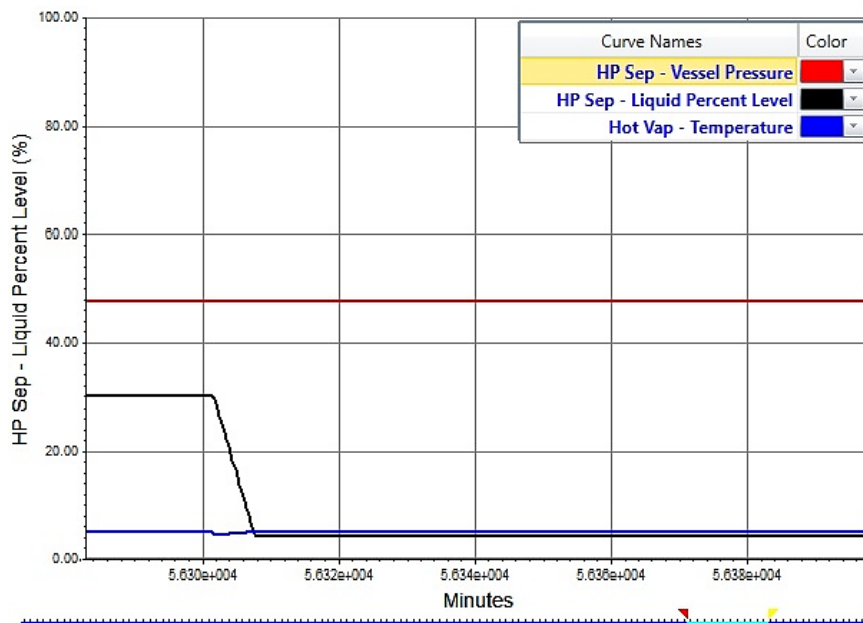


Figure 4.6. Valve VLV- 102 actuators have failed open strip chart.



### Scenario 2. Valve actuator Failed Close.

For the node “Valve Actuator Failed Shut” the Aspen Hysys Dynamics Simulation was run given the Actuator has Failed Shut scenario for valve VLV-102. After the valve VLV-102 failed close, the liquid level in tank reached 95.35 %. The outcome is displayed in the form of the strip chart. Based on the obtained results and eqn 4.3, the POF was estimated as:

$$POF_2 = \frac{\text{Malfunction time range}}{\text{total operational time}} = \frac{57480 \text{ min} - 57180 \text{ min}}{57480 \text{ min} - 57080 \text{ min}} = \frac{300 \text{ min}}{400 \text{ min}} = 0.75$$

### Scenario 3. Selecting the wrong switch for the application

For the node “Selecting the wrong switch for your application” the action of the level controller of valve VLV-102 was set to reverse instead of the direct (Figure 4.7). Resultantly the liquid level in the separator dropped from 30 % to 4.18 %. The POF for this scenario was then estimated and the result was inserted into the conditional probability table (CPT) of the corresponding node in the DBN model in Genie.

$$POF_3 = \frac{\text{Malfunction time range}}{\text{Total operational time}} = \frac{60888 \text{ min} - 60366 \text{ min}}{60888 \text{ min} - 59689 \text{ min}} = \frac{522 \text{ min}}{1199 \text{ min}} = 0.435$$

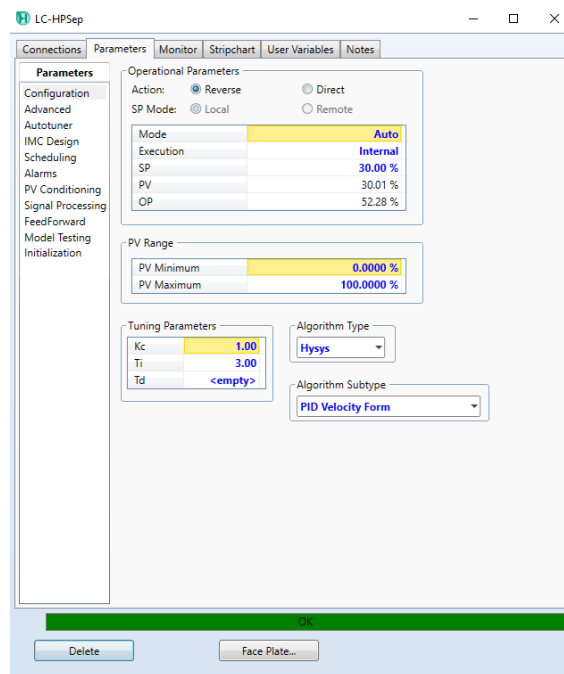


Figure 4.7. Level controller incorrectly set-up due to wrong switch selection.

#### Scenario 4. Heat introduction and fire mitigation scenario

In this scenario, the POF is estimated for node "Adding valve and interlock at the inlet stream of the separator" given fire in the two-phase separator (Figure 4.8). The heat was introduced to the vessel and with the employment of the event scheduler and cause and effect matrix, the closing of the all of the valves during the fire extinguishing was simulated with subsequent fire relief via the pressure safety valves before the pressure is returned to the normal operating pressure. After that, the closed valves were opened, and the operation continued at the recovered conditions.

The normal operational pressure range for this scenario was the pressure range of 490-520 kPa. The valves VLV-100, VLV-101 and VLV-102 were set to close at the pressure of 655 kPa. Based on the analysis of the obtained strip charts the disruption is seen to start at time 100499 seconds and finishes at 111904 seconds, whereas the whole operation starts, and finish time is 96297 seconds and 117014 seconds, respectively.

$$POF_4 = \frac{\text{Malfunction time range}}{\text{Total operational time}} = \frac{111904 \text{ sec} - 100499 \text{ sec}}{117014 \text{ sec} - 96297 \text{ sec}} = \frac{11405 \text{ sec}}{20717 \text{ sec}} = 0.551$$

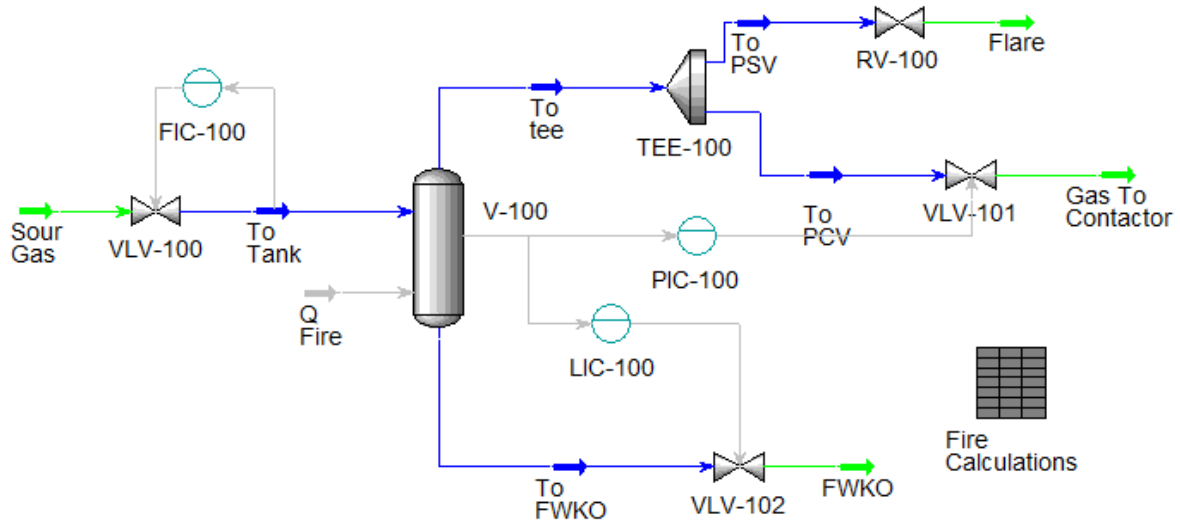


Figure 4.8. Simulation of fire in the 2-phase separator

Inserting the POFs obtained via the simulation, the resilience curve for the 2-phase separator is obtained. Figure 4.9 presents the resilience of the separator given the disruption in terms of the malfunctions that may occur due to inaccurate performance or too late a response of the level alarm and interlock systems or the operator working in the control room.

It takes 9 hours for disruption to bring the separator to the lowest level of the state of functionality, i.e., 0.48. Furthermore, it takes 56 hours for the system to restore to 0.94 – the highest state of functionality after the adaptation and restoration measures applied to the separator.

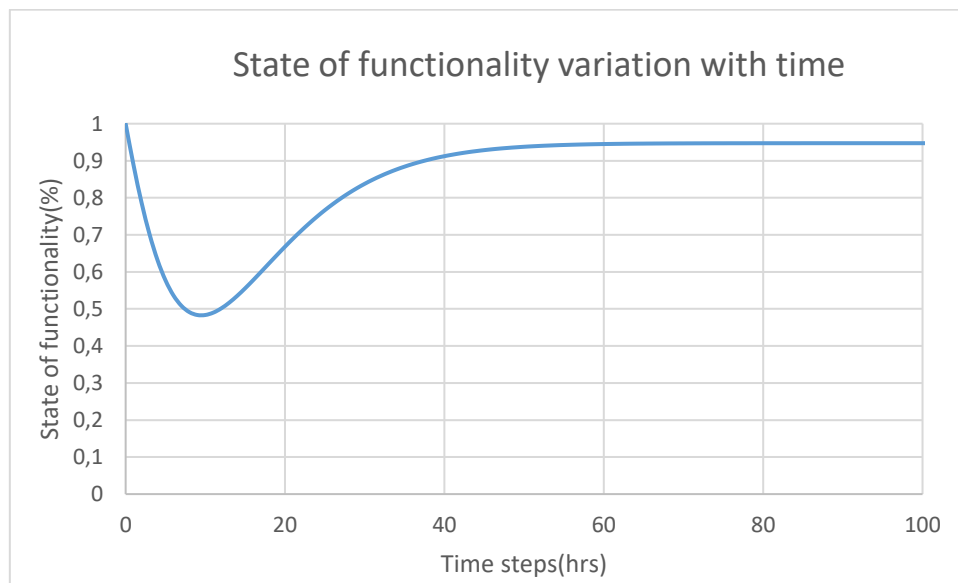


Figure 4.9. The Resilience curve

Additional nodes were considered for “Absorption”, “Adaptation” and “Restoration” (Table 4.6). This was done to build a more resilient DBN model for the two-phase separator and at the same time for validation of the DBN model developed previously (Figure 4.4). With the additional nodes, the resilience profile is expected to enhance. In case the resilience profile displays stronger “Absorption”, “Adaptation” and “Restoration” characteristics, the structure of the DBN model can be validated.

Table 4.6. Additional safety measures for the DBN model (Figure 4.4)

Absorption	Additional Operator at the control room
Adaptation	Bypass Valves
	Relief Valves
Restoration	Replacement of the damaged valves
	The pay bonus system for the safe month

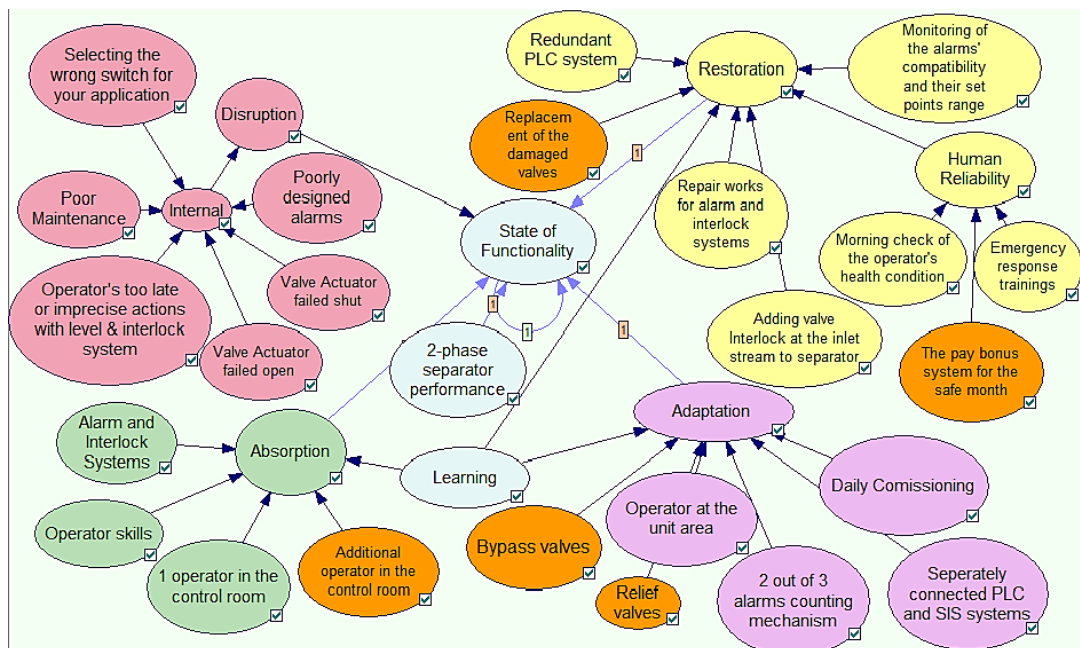


Figure 4.10. Updated DBN model with the additional parameters (orange nodes) presented in Table 6.

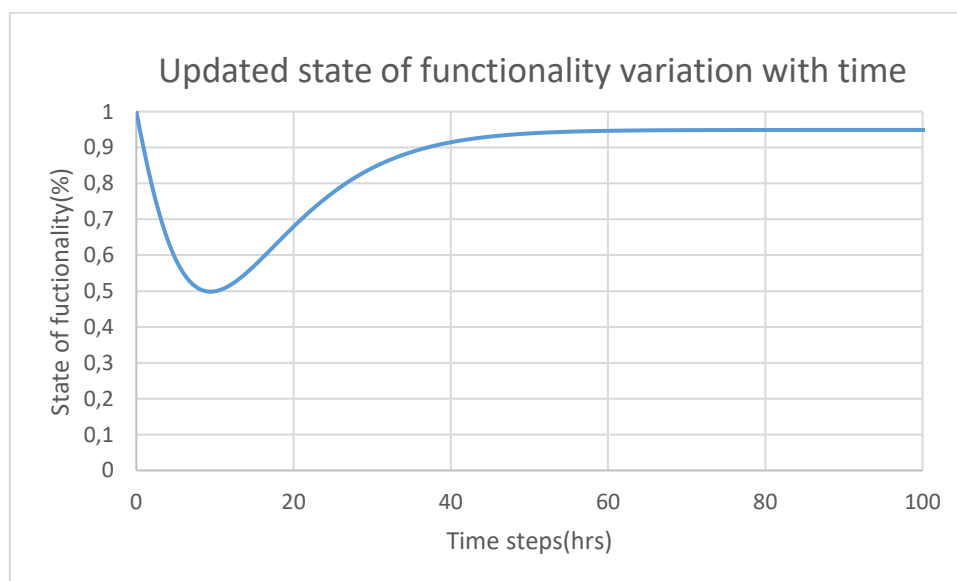


Figure 4.11 The resilience model of the system with additional resilience parameters

Table 4.7. Comparison of resilience metrics

<b>Resilience metrics</b>	<b>DBN Model1 (Figure 3.4)</b>	<b>DBN Model 2 (Figure 3.6)</b>
Disruption occurrence time (hrs)	9	9
Resilience decline value (%)	48.34%	50.0%
The probability of the final resilient state S4 (%)	94.32%	94.83%
Time for resilience stabilization (hrs)	56	56
Time for 90 % recovery (hrs)	38	37

From a comparison of the DBN models in Table 4.7, it is observed that the lowest value of resilience has increased from 48.34% to 50.00% with the addition of the new parameter for the "Absorption" node. This designated the stronger absorption properties of the system. The probability of the final resilient state is slightly increased at the updated DBN model and the time for 90 % recovery is shorter than in the initial DBN model. Both characteristics are evidence of the strengthening of the "Adaptation" and "Restoration" parameters of the system. Thus, the DBN model is validated.

#### 4.2.4 Sensitivity Analysis in Genie Simulation for identification of the most influential nodes

Sensitivity analysis was carried out to identify the nodes having the highest impact on the state of the system's functionality. Identification of the critical nodes assists in the allocation of specialized safety measures to the system. Table 4.8 lists 11 scenarios, each representing a high error probability state or low functional state contributing to the variation of the resilience of the system.

Table 4.8. Scenarios for sensitivity analysis

Scenario 1	Low absorption
Scenario 2	Not functioning alarm and interlock systems
Scenario 3	Poor operator skills
Scenario 4	The low learning ability of the system
Scenario 5	Low 2-phase separator performance
Scenario 6	High disruption
Scenario 7	No properly functioning redundant PLC system
Scenario 8	No repair works for alarm and interlock systems
Scenario 9	Low human reliability
Scenario 10	No morning check of the operators' health condition
Scenario 11	No emergency response training

Table 4.9. The results of sensitivity analysis

Scenarios	Resilience Reduction(%)	Time to reach lowest reliability(hrs)	Time for 90% recovery (hrs)
1	0.27	2	21
2	36.71	8	28
3	34.39	8	28
4	42.81	8	30
5	47.41	9	31
6	48.83	10	32
7	48.8	9	32
8	48.32	9	32
9	45.55	11	32
10	47.75	10	32
11	47.87	10	32

From Table 4.9 it can be seen that the highest impact on the resilience drop occurs at low absorption conditions, however, with the strong adaptation and restoration characteristics the system restores to the normal operational state (90% of recovery) at the shortest amount of time than in the other scenarios. The highest impact on the resilience drop is done under the effect of the poor operator skills and not functioning alarm and interlock system. Scenarios 4-11 show the resilience reduction to the value around 40 % in approximately 9 hours which represent the strong absorption properties or well-thought inherent safety design of the developed model.

#### ***4.2.5 The Worn-Out Separator Resilience Assessment***

The resilience of the separator was assessed after 2,000 hours of work, according to Liao,2011, which is equal to 70.36 %. The nodes of the Resilience Dynamic Bayesian Network model were updated according to the calculated reliability. After the nodes being updated, the dynamic resilience profile was obtained. The previous reliabilities of the node "Alarm and Interlock System", "Bypass valves", "Relief valves" , "2 phase separator performance", "2 out of 3 alarm counting mechanism", "Separately connected PLC and SIS systems", "Poorly designed alarms", "Valve actuator failed shut", "Valve actuator failed open" were multiplied by 0.7036. The probabilities of failures were updated for the nodes of absorption, adaptation, and disruption and "2-phase separator performance" nodes.

The state of the functionality of the separator is dropped in 7 hours, and after the restoration, the resilience of the separator reached a stable value of 88% after 45 hours. Thus,

although it took a shorter amount of time for the state of functionality to drop, the system managed to recover to the high operational state at the same amount of time as in the case of the separator performance without the equipment being a worn-out assumption.

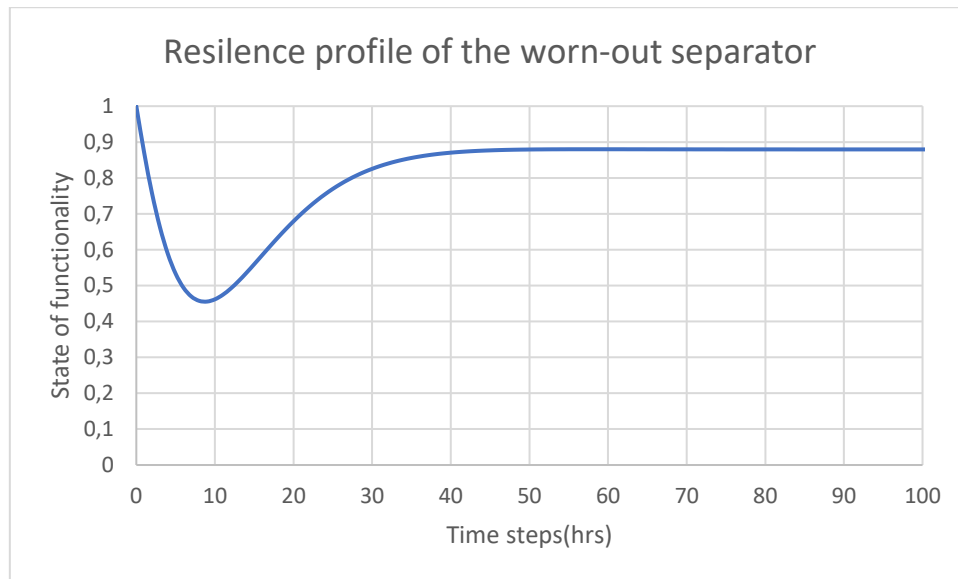


Figure 4.12. The resilience profile of the worn-out separator.

Overall, the case study demonstrated the applicability and effectiveness of the integration of the FRAM and DBN for quantitative resilience assessment of complex process systems consisting of the socio-technical aspects.



# Chapter 5- Conclusion and Future Work

The Dynamic Quantitative Resilience Assessment of the process systems is the new direction in the sphere of resilience engineering. The complexity of the process plants requires the rigorous analysis of the root causes of the accidents and mishaps as well as the resilience attributes of the process systems on the level of socio-technical interactions. Additionally, the highly uncertain harsh cold environments and their impacts on process systems' performance, and the lack of operational experience and historical data make a risk assessment of process operations more challenging. For process systems operating in harsh environments, resilience assessment is more suitable as it can better deal with uncertain events during pre-disruption and post-disruption stages.

Throughout this study the resilience assessment on the two-phase separator of acid gas sweetening unit was conducted for the two cases:

- Case 1: The possible threats for the two-phase separator were identified by application of FRAM and Monte Carlo Simulation. The resilience assessment was further conducted by development of four main resilience attributes corresponding to those threats.
- Case 2: The dynamic quantitative resilience assessment was conducted for the known threat, which was analyzed for possible causes and consequences using the BT. The BT was then transferred into the DBN to assess the temporal evolution of the state of functionality of the system.

For both case studies the Sensitivity analysis was conducted and the critical factors enhancing the system resilience were identified. Furthermore, the resilience variation with temporal equipment degradation was analyzed via employing Weibull Distribution.

The main deliverables of this research work are:

- Inclusion of both the subjective and objective data for estimation of the state of functionality in DBN
- Identification of the root causes of the accident development scenario and the possible system response to it with the BT. Integration with DBN to assess the current resilience

and the evolution of the resilience after the disruption and with the adaptation, restoration, and learning parameters.

- The identification of the critical connections between socio-technical interactions that may potentially cause the accident development with FRAM. Integration of FRAM with DBN for assessment of the current resilience state of the system and the evolution of the resilience with restoration and learning.
- The study proves that resilience should be assessed in both probabilistic and temporal terms.
- It investigates the usefulness of process simulators as a process data source for PoF estimation.
- It highlights the effectiveness of the DBN model for identification of the most influential safety measures.
- Overall, the case study proved that the proposed method could generate a dynamic resilience profile, which could assist in the estimation of systems' capability to withhold uncertain disruptions, monitoring their performance variation, assessing the effectiveness of safety measures, and identification of potential design and operational improvements.

The limitations of the study were inability to access the plant data for obtaining and validation of the POF values.

For future work, I will suggest integrating the machine learning and deep learning approaches to replace the subjective POF data and make the outcomes more accurate. For this purpose, I will suggest application of artificial neural networks (ANN) for some available data set, to further generate more values and estimation of POF out of approximately 10,000 outputs generated with ANN.

Furthermore, I will suggest validating the cumulative variability outcomes obtained with integration of FRAM and MCS, by running MCS for 500, 2000, and 3000 iterations.

# Bibliography

- Adger, W. N. (2000). Social and ecological resilience: are they related? *Progress in Human Geography*, 24(3), 347–364. doi: 10.1191/030913200701540465
- Azadeh, A., Salehi, V., Arvan, M., & Dolatkhah, M. (2014). Assessment of resilience engineering factors in high-risk environments by fuzzy cognitive maps: A petrochemical plant. *Safety Science*, 68, 99-107.
- Baroud, H., Ramirez-Marquez, J. E., Barker, K., & Rocco, C. M. (2014a). Stochastic measures of network resilience: Applications to waterway commodity flows. *Risk Analysis*, 34(7), 1317-1335.
- Baroud, H., Barker, K., & Ramirez-Marquez, J. E. (2014b). Importance measures for inland waterway network resilience. *Transportation research part E: logistics and transportation review*, 62, 55-67.
- Berkeley, A. R., Wallace, M., & COO, C. (2010). A framework for establishing critical infrastructure resilience goals. Final Report and Recommendations by the Council, National Infrastructure Advisory Council.
- Birolini, A. (2013). *Reliability engineering: theory and practice*. Springer Science & Business Media.
- Burnard, K., & Bhamra, R. (2011). Organisational resilience: development of a conceptual framework for organisational responses. *International Journal of Production Research*, 49(18), 5581–5599. doi: 10.1080/00207543.2011.563827
- Cai, B., Xie, M., Liu, Y., Liu, Y., & Feng, Q. (2018). Availability-based engineering resilience metric and its corresponding evaluation methodology. *Reliability Engineering & System Safety*, 172, 216-224.
- Cai, B., Shao, X., Liu, Y., Kong, X., Wang, H., Xu, H., & Ge, W. (2019). Remaining useful life estimation of structure systems under the influence of multiple causes: Subsea pipelines as a case study. *IEEE Transactions on Industrial Electronics*.
- Costella, M. F., Saurin, T. A., & Guimarães, L. B. D. M. (2009). A method for assessing health and safety management systems from the resilience engineering perspective. *Safety Science*, 47(8), 1056–1067. doi: 10.1016/j.ssci.2008.11.006
- Dinh, L. T., Pasman, H., Gao, X., & Mannan, M. S. (2012). Resilience engineering of industrial processes: principles and contributing factors. *Journal of Loss Prevention in the Process Industries*, 25(2), 233-241.
- Faturechi, R., & Miller-Hooks, E. (2014). Travel time resilience of roadway networks under disaster. *Transportation research part B: methodological*, 70, 47-64.
- Fiksel, J. (2006). Sustainability and resilience: toward a systems approach. *Sustainability: Science, Practice and Policy*, 2(2), 14–21. doi: 10.1080/15487733.2006.11907980
- GeNIe Modeler – BayesFusion. (n.d.). Retrieved from <https://www.bayesfusion.com/genie>
- Holling, C. S. (1973). Resilience and Stability of Ecological Systems. *Annual Review of Ecology and Systematics*, 4(1), 123. <https://doi.org/10.1146/annurev.es.04.110173.000245>
- Hollnagel, E. (2012). *FRAM, the functional resonance analysis method: modelling complex socio-technical systems*. Ashgate Publishing, Ltd..
- Hollnagel, E., Woods, D., & Leveson, N. (2006). Resilience Engineering : Concepts and Precepts. *Resilience Engineering: Concepts and Precepts*.
- Hosseini, S., & Barker, K. (2016). Modeling infrastructure resilience using Bayesian networks: A case study of inland waterway ports. *Computers & Industrial Engineering*, 93, 252-266.
- HYSYS, A. (2004). Release 2004, simulation basis. Aspen Technology, Cambridge, MA.

- Jain, P., Pasman, H. J., Waldram, S., Pistikopoulos, E. N., & Mannan, M. S. (2018). Process Resilience Analysis Framework (PRAF): A systems approach for improved risk and safety management. *Journal of Loss Prevention in the Process Industries*, 53, 61-73.
- Jensen, F. V., & Nielsen, T. D. (2007). Bayesian Networks and Decision Graphs. *Information Science and Statistics*. doi: 10.1007/978-0-387-68282-2
- Kammouh, O., Gardoni, P., & Cimellaro, G. P. (2020). Probabilistic framework to evaluate the resilience of engineering systems using Bayesian and dynamic Bayesian networks. *Reliability Engineering & System Safety*, 198, 106813.
- Kendra, J. M., & Wachtendorf, T. (2003). Elements of Resilience After the World Trade Center Disaster: Reconstituting New York City's Emergency Operations Centre. *Disasters*, 27(1), 37–53. doi: 10.1111/1467-7717.00218
- Khakzad, N. (2015). Application of dynamic Bayesian network to risk analysis of domino effects in chemical infrastructures. *Reliability Engineering & System Safety*, 138, 263–272. doi:10.1016/j.ress.2015.02.007
- Kinzig, A. P., Ryan, P., Etienne, M., Allison, H., Elmqvist, T., & Walker, B. H. (2006). Resilience and Regime Shifts: Assessing Cascading Effects. *Ecology and Society*, 11(1). doi: 10.5751/es-01678-110120
- Li, Y., & Lence, B. J. (2007). Estimating resilience for water resources systems. *Water Resources Research*, 43(7).
- Liao, Q., Wang, X., Ling, D., Xiao, Z., & Huang, H. Z. (2011, June). Equipment reliability analysis based on the Mean-rank method of two-parameter Weibull distribution. In 2011 *International Conference on Quality, Reliability, Risk, Maintenance, and Safety Engineering* (pp. 361-364). IEEE.
- Luthar, S. S., Cicchetti, D., & Becker, B. (2000). The Construct of Resilience: A Critical Evaluation and Guidelines for Future Work. *Child Development*, 71(3), 543–562. doi: 10.1111/1467-8624.00164
- McCarthy, J. A. (2007). Introduction: from protection to resilience: injecting 'Moxie' into the infrastructure security continuum. *Critical Thinking: Moving from Infrastructure Protection to Infrastructure Resilience*, 2-3.
- Naseri, M. (2017). On Maintainability of Winterised Plants Operating in Arctic Regions. In *ASME 2017 36th International Conference on Ocean, Offshore and Arctic Engineering*. American Society of Mechanical Engineers Digital Collection.
- Neapolitan, R., & Jiang, X. (2007). Learning Bayesian Networks. *Probabilistic Methods for Financial and Marketing Informatics*, 111–175. doi: 10.1016/b978-012370477-1/50021-9
- Noroozi, A., Abbassi, R., MacKinnon, S., Khan, F., & Khakzad, N. (2014). Effects of cold environments on human reliability assessment in offshore oil and gas facilities. *Human factors*, 56(5), 825-839.
- Ossai, C. I., Boswell, B., & Davies, I. J. (2015). Estimation of internal pit depth growth and reliability of aged oil and gas pipelines—A Monte Carlo simulation approach. *Corrosion*, 71(8), 977-991.
- Park, J., Seager, T. P., Rao, P. S. C., Convertino, M., & Linkov, I. (2013). Integrating risk and resilience approaches to catastrophe management in engineering systems. *Risk Analysis*, 33(3), 356-367.
- Patriarca, R., Di Gravio, G., & Costantino, F. (2017). A Monte Carlo evolution of the Functional Resonance Analysis Method (FRAM) to assess performance variability in complex systems. *Safety science*, 91, 49-60.
- Patriarca, R., Bergström, J., & Di Gravio, G. (2017). Defining the functional resonance analysis space: Combining Abstraction Hierarchy and FRAM. *Reliability Engineering & System Safety*, 165, 34–46. <https://doi.org/https://doi.org/10.1016/j.ress.2017.03.032>
- Patriarca, R., Di Gravio, G., Costantino, F., & Tronci, M. (2017). The Functional Resonance

- Analysis Method for a systemic risk based environmental auditing in a sinter plant: A semi-quantitative approach. *Environmental Impact Assessment Review*, 63, 72–86.  
<https://doi.org/10.1016/j.eiar.2016.12.002>
- Perrings, C. (2006). Resilience and sustainable development. *Environment and Development Economics*, 11(4), 417–427. doi: 10.1017/s1355770x06003020
- Podofillini, L., Sudret, B., Stojadinovic, B., Zio, E., & Kröger, W. (Eds.). (2015). *Safety and Reliability of Complex Engineered Systems: ESREL 2015*. CRC press.
- Pomeroy, J. W., & Li, L. (2000). Prairie and arctic areal snow cover mass balance using a blowing snow model. *Journal of Geophysical Research: Atmospheres*, 105(D21), 26619–26634.
- Rosa, L. V., Haddad, A. N., & de Carvalho, P. V. R. (2015). Assessing risk in sustainable construction using the Functional Resonance Analysis Method (FRAM). *Cognition, Technology & Work*, 17(4), 559–573.
- Rose, A., & Liao, S.-Y. (2005). Modeling Regional Economic Resilience to Disasters: A Computable General Equilibrium Analysis of Water Service Disruptions\*. *Journal of Regional Science*, 45(1), 75–112. doi: 10.1111/j.0022-4146.2005.00365.x
- Shirali, G. A., Mohammadfam, I., & Ebrahimipour, V. (2013). A new method for quantitative assessment of resilience engineering by PCA and NT approach: A case study in a process industry. *Reliability Engineering & System Safety*, 119, 88–94.
- Shirali, G. A., Ebrahimipour, V., & Mohamm Salahi, L. (2013). Proactive risk assessment to identify emergent risks using functional resonance analysis method (fram): a case study in an oil process unit. *Iran Occupational Health*, 10(6).
- Steen, R., & Aven, T. (2011). A risk perspective suitable for resilience engineering. *Safety science*, 49(2), 292–297.
- Tian, J., Wu, J., Yang, Q., & Zhao, T. (2016). FRAMA: a safety assessment approach based on Functional Resonance Analysis Method. *Safety science*, 85, 41–52.
- Tong, Q., Yang, M., Zinetullina, A. “A Dynamic Bayesian Network-based Approach to Resilience Assessment of Engineered Systems,” submitted to *Journal of Loss Prevention in the Process Industries*, March. 2020 (under review).
- Trautwine, J. C. (1919). *The civil engineer's pocket-book*. Thomas Telford Publishing.  
<https://doi.org/doi:10.1680/tcepb20e2i.52208>
- Vogel, R. M., & Bolognese, R. A. (1995). Storage-reliability-resilience-yield relations for over-year water supply systems. *Water Resources Research*, 31(3), 645–654.
- Vugrin, Eric D., et al. “A Framework for Assessing the Resilience of Infrastructure and Economic Systems.” *Sustainable and Resilient Critical Infrastructure Systems*, 2010, pp. 77–116., doi:10.1007/978-3-642-11405-2\_3.
- Yang, M., Khan, F. I., Lye, L., Sulistiyono, H., Dolny, J., & Oldford, D. (2013). Risk-based winterization for vessels operations in Arctic environments. *Journal of Ship Production and Design*, 29(4), 199–210.
- Yodo, N., Wang, P., & Zhou, Z. (2017). Predictive resilience analysis of complex systems using dynamic Bayesian networks. *IEEE Transactions on Reliability*, 66(3), 761–770.
- Zhang, L., Wu, S., Zheng, W., & Fan, J. (2018). A dynamic and quantitative risk assessment method with uncertainties for offshore managed pressure drilling phases. *Safety science*, 104, 39–54.
- Zinetullina, A., Yang, M., Khakzad, N., & Golman, B. (2019). Dynamic resilience assessment for process units operating in Arctic environments. *Safety in Extreme Environments*, 1–13.